The Plant Cell, Vol. 28: 1860–1878, August 2016, www.plantcell.org

Regulation of Leaf Starch Degradation by Abscisic Acid Is Important for Osmotic Stress Tolerance in Plants[OPEN]

Matthias Thalmann,[a] Diana Pazmino,[a] David Seung,[b] Daniel Horrer,[a] Arianna Nigro,[a] Tiago Meier,[a] Katharina Kölling,[b] Hartwig W. Pfeifhofer,[c] Samuel C. Zeeman,[b] and Diana Santelia[a,1]

[a] Department of Plant and Microbial Biology, University of Zürich, 8008 Zürich, Switzerland
[b] Institute for Agricultural Sciences, ETH Zürich, 8092 Zürich, Switzerland
[c] Institut für Pflanzenwissenschaften, Karl-Franzens-Universität Graz, 8010 Graz, Austria

ORCID IDs: 0000-0002-2572-2603 (K.K.); 0000-0002-4201-4502 (H.P.)

Starch serves functions that range over a timescale of minutes to years, according to the cell type from which it is derived. In guard cells, starch is rapidly mobilized by the synergistic action of β-AMYLASE1 (BAM1) and α-AMYLASE3 (AMY3) to promote stomatal opening. In the leaves, starch typically accumulates gradually during the day and is degraded at night by BAM3 to support heterotrophic metabolism. During osmotic stress, starch is degraded in the light by stress-activated BAM1 to release sugar and sugar-derived osmolytes. Here, we report that AMY3 is also involved in stress-induced starch degradation. Recently isolated *Arabidopsis thaliana amy3 bam1* double mutants are hypersensitive to osmotic stress, showing impaired root growth. *amy3 bam1* plants close their stomata under osmotic stress at similar rates as the wild type but fail to mobilize starch in the leaves. ^{14}C labeling showed that *amy3 bam1* plants have reduced carbon export to the root, affecting osmolyte accumulation and root growth during stress. Using genetic approaches, we further demonstrate that abscisic acid controls the activity of BAM1 and AMY3 in leaves under osmotic stress through the AREB/ABF-SnRK2 kinase-signaling pathway. We propose that differential regulation and isoform subfunctionalization define starch-adaptive plasticity, ensuring an optimal carbon supply for continued growth under an ever-changing environment.

INTRODUCTION

Starch is the most abundant form in which plants store carbohydrates. Its metabolism and function depends upon the cell type from which it is derived. In guard cells, starch is present at night and degraded within 30 min of light to promote rapid stomatal opening (Horrer et al., 2016; Blatt, 2016). In the leaves, starch typically accumulates gradually during the day using a fraction of the carbon assimilated through photosynthesis. At night, the starch that was synthesized the previous day is almost precisely consumed at dawn for continued sucrose biosynthesis and energy production when photosynthesis does not occur, a process vital for plant growth (Smith and Stitt, 2007; Stitt and Zeeman, 2012; Scialdone and Howard, 2015; Graf and Smith, 2011). Mutant *Arabidopsis thaliana* plants that fail to synthesize or degrade starch in the leaves have reduced growth rates under most conditions (Yazdanbakhsh and Fisahn, 2011; Usadel et al., 2008b). This nearly linear pattern of starch biosynthesis and degradation is retained under changing photoperiods or if plants are subject to a sudden early or late dusk, as long as the total circadian rhythm remains at 24 h (Sulpice et al., 2014; Graf et al., 2010). It is indeed observed that plants degrade starch faster in long days than in short days, demonstrating that plants somehow anticipate the length on the following night (Gibon et al., 2004; Lu et al., 2005). Such a tight regulation of starch degradation rates prevents carbon starvation or nonproductive carbon sequestration, thereby supporting continued growth during the night (Stitt and Zeeman, 2012).

Evidence is accumulating for an analogous adaptive response of leaf starch metabolism to other challenges, such as a severe water deficit or extreme temperatures. In response to acute temperature shock, plants mobilize starch at time when biosynthesis would be expected (e.g., in the middle of the light period), resulting in the accumulation of maltose, the major starch catabolite, and of its deriving sugars (Usadel et al., 2008a; Purdy et al., 2013; Kaplan and Guy, 2005, 2004; Sitnicka and Orzechowski, 2014; Yano et al., 2005; Kaplan et al., 2007). Similar rearrangements of starch metabolism are observed when plants are subject to short periods of oxidative or osmotic stress (Scarpeci and Valle, 2008; Zanella et al., 2016; Valerio et al., 2011; Geigenberger et al., 1997). It is proposed that soluble sugars and other charged metabolites, such as proline or glycine, may function as osmoprotectants during stress responses. Stress-induced accumulation of these metabolites lowers the water potential of the cell, promoting water retention in the plant without interfering with normal metabolism. This process, known as osmotic adjustment, enables the maintenance of cell turgor for plant growth and survival under stress conditions (Bartels and Sunkar, 2005; Verslues and Sharma, 2011; Krasensky and Jonak, 2012). Sugars and proline can also help stabilize proteins and cell structures, particularly when the stress becomes severe or persists for

[1] Address correspondence to dsantelia@botinst.uzh.ch.
The author responsible for distribution of materials integral to the findings presented in this article in accordance with the policy described in the Instructions for Authors (www.plantcell.org) is: Diana Santelia (dsantelia@botinst.uzh.ch).
[OPEN]Articles can be viewed without a subscription.
www.plantcell.org/cgi/doi/10.1105/tpc.16.00143

longer periods (Hoekstra et al., 2001). These compounds can also act as free radical scavengers, protecting against oxidation by removing excess reactive oxygen species, reestablishing the cellular redox balance (Couée et al., 2006; Miller et al., 2010). Thus, the ability to adjust patterns of assimilation, storage, and utilization of carbon in response to changes in the environment may determine not only biomass production but also plant fitness in terms of survival under stressful environmental conditions. Despite its importance, our understanding of how carbon is provided for metabolism and growth under stress is poor.

Transitory starch degradation at night begins with the phosphorylation of the glucan chains by glucan, water dikinase (GWD) and phosphoglucan, water dikinase (PWD) (Ritte et al., 2006). The chains are then simultaneously degraded by a set of glucan-hydrolyzing enzymes (including β-amylases [BAM], α-amylases [AMY], and debranching enzymes) and dephosphorylated by phosphoglucan phosphatases (Streb and Zeeman, 2012). These enzymes work in synergy to completely degrade starch (Kötting et al., 2009; Edner et al., 2007). Hydrolysis of starch to maltose by BAM represents the predominant pathway of transitory starch degradation. BAM3 is the major isoform in the nighttime leaf starch metabolism, and Arabidopsis *bam3* mutants have elevated amounts of starch and reduced levels of maltose at night compared with the wild type (Fulton et al., 2008; Kaplan and Guy, 2005). BAM1 is highly expressed in guard cells and, in synergy with AMY3, degrades starch in these cells for light-induced stomatal opening (Horrer et al., 2016; Blatt, 2016). Under osmotic stress, BAM1 is activated in the leaves and contributes to diurnal starch degradation for sugars and proline biosynthesis (Valerio et al., 2011; Zanella et al., 2016). Thus, it appears that BAM1 is important for stress-induced leaf starch degradation. However, it is unclear if other starch hydrolytic enzymes also play a role during stress, how the process is controlled, and what the significance is for plant stress tolerance.

To address these questions, we subjected hydroponically grown Arabidopsis plants to a short-term, high osmotic stress and show that AMY3 is also involved in stress-induced starch degradation. Mutants lacking both BAM1 and AMY3 are sensitive to osmotic stress. This is because in the absence of these two enzymes, plants fail to mobilize starch in the leaves during stress and have reduced carbon export to the root, affecting osmolyte accumulation for water and nutrient uptake and root growth. We also show that the stress hormone abscisic acid (ABA) controls the activity of BAM1 and AMY3 during stress responses, and we provide evidence that the mechanism we describe for Arabidopsis is most likely conserved among different plant species. Our discovery uncovers a critical function for starch in plant stress tolerance and highlights BAM1 and AMY3 as targets for breeding stress-tolerant crops.

RESULTS

BAM1 and AMY3 Synergistically Degrade Starch in Leaves upon Osmotic Stress

To study the effects of osmotic stress on starch metabolism, we subjected 3-week-old Arabidopsis plants grown in hydroponic culture to 300 mM mannitol treatment for 4 h, starting after 3 h of light. The plants visibly wilted but, when returned to control solution without mannitol for 24 h, they recovered fully (Figure 1A). After 4 h of stress, wild-type plants accumulated 51% less starch compared with control plants (Figure 1B). The reduced accumulation of starch was accompanied by a significant accumulation of maltose to levels comparable to, or higher than, those normally observed at night (Figure 1C) (Fulton et al., 2008). The plants responded in a similar way when the osmotic stress was imposed using 300 mM sorbitol (Supplemental Figure 1). The Arabidopsis mutant *phosphoglucomutase* (*pgm*), which is devoid of starch (Caspar et al., 1985), accumulated tiny amounts of maltose during the day under control growth conditions. However, in response to osmotic stress, the maltose levels in *pgm* remained unchanged (Supplemental Figure 2). Thus, the reduction in starch accumulation in osmotically stressed plants appeared, at least in part, to result from starch turnover (i.e., simultaneous biosynthesis and degradation).

BAM1 gene expression was induced 8-fold in wild-type leaves upon mannitol treatment, similar to *RD29A*, a well-known osmotic stress-responsive gene (Figure 1D) (Yamaguchi-Shinozaki and Shinozaki, 1994). *bam1* mutant plants showed reduced osmotic stress-induced starch degradation and maltose accumulation but were indistinguishable from the wild type under control conditions (Figures 1B and 1C; Supplemental Figure 3). In contrast, *BAM3* transcripts were not induced by mannitol (Figure 1D), and *bam3* mutants, despite having elevated starch levels compared with the wild type, activated starch degradation similarly to the wild type (Figures 1B and 1C; Supplemental Figure 3). *BAM1* gene expression was stress-induced in *bam3* mutants to the same extent as in the wild type (14-fold in this experiment; Supplemental Figure 4), suggesting that BAM1 is activated in *bam3* to promote starch mobilization during the osmotic stress response. These results indicate that BAM1 and BAM3 are critical under different conditions.

The finding that BAM1 degrades starch synergistically with AMY3 (Seung et al., 2013; Horrer et al., 2016) prompted us to investigate the relevance of this interaction during osmotic stress responses. Like *bam1*, the *amy3* mutant appears similar to the wild type under standard growth conditions (Supplemental Figure 3) (Yu et al., 2005). However, upon stress, *amy3* mutants showed a reduction in starch degradation and reduced maltose accumulation relative to the wild type, showing that AMY3 is also required for starch degradation under osmotic stress (Figures 1B and 1C). The defects in *amy3* were not as severe as those in *bam1*. qPCR analysis of *AMY3* expression under osmotic stress showed that there was a small induction after 4 h of mannitol treatment (Figure 1D). This induction was in addition to the previously described increase in AMY3 transcript that occurs during the day (apparent in our control plants; Figure 1D; Supplemental Figure 5A) (Smith et al., 2004). Loss of both AMY3 and BAM1 proteins in the *amy3 bam1* double mutant did not alter starch levels under osmotic stress, with starch accumulating to the same extent as in unstressed plants (Figures 1B and 1C). However, starch metabolism under control conditions was not affected in this mutant (Supplemental Figure 3) (Horrer et al., 2016). These results suggest that BAM1 and AMY3 are both induced during osmotic stress and work together to mediate efficient starch catabolism in the leaves.

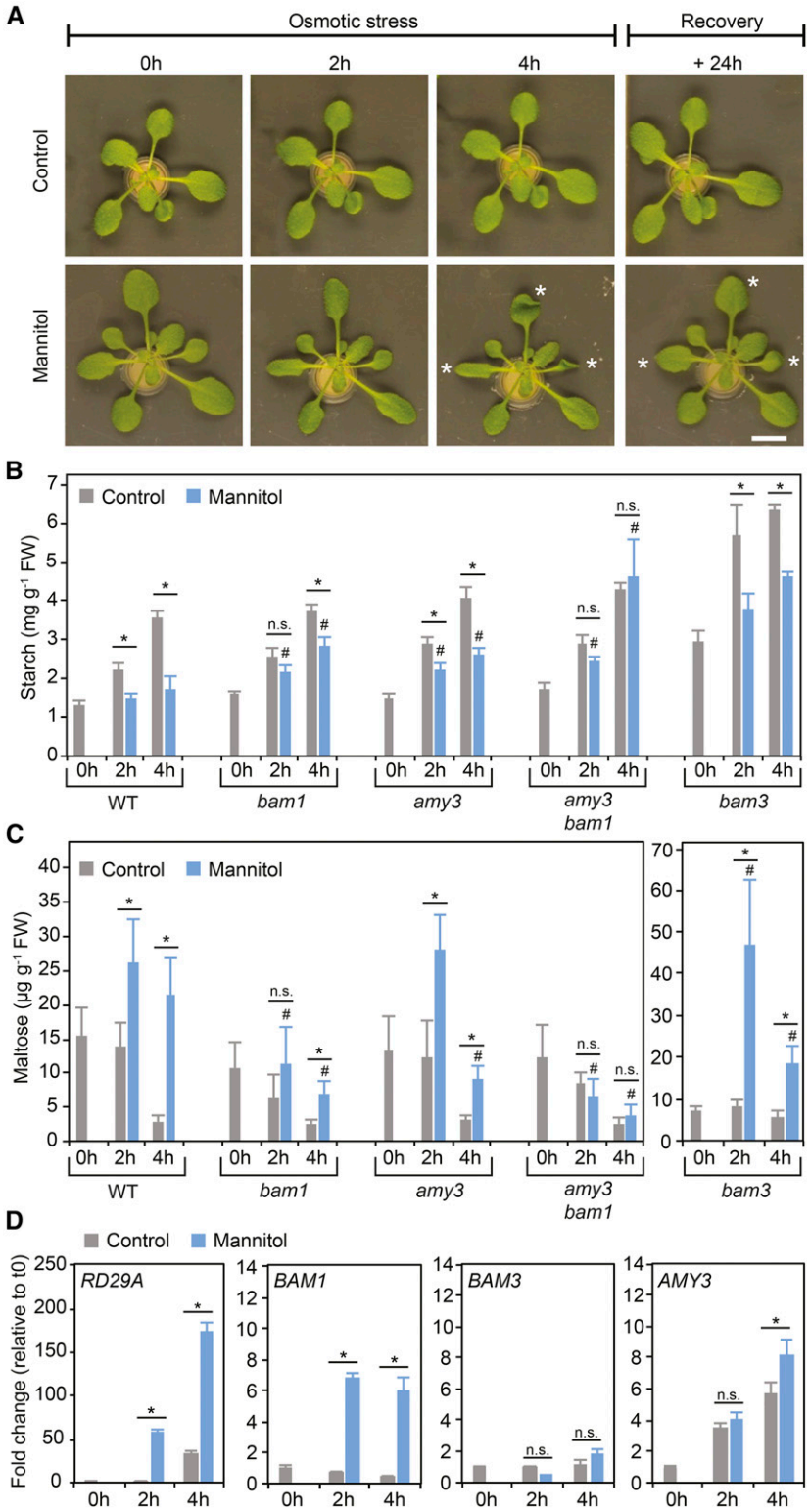

Figure 1. Leaf Starch Levels during Osmotic Stress Are Unchanged in *amy3 bam1* Mutant Plants.

(A) Three-week-old hydroponically grown Arabidopsis plants were transferred to a nutrient solution optionally supplemented with 300 mM mannitol for 4 h. After the stress treatment, roots were rinsed with water and returned to a control solution for 24 h. Representative wild-type plants (Col-0) show the reduction in turgor in response to mannitol stress (denoted by asterisks) from which the plants recovered after 24 h in control nutrient solution. Bar = 1 cm.

Simultaneous Loss of BAM1 and AMY3 Affects Osmotic Stress Tolerance

To investigate the importance of starch degradation in osmotic stress tolerance, we examined *amy3 bam1* performance under stress. Measurements of leaf relative water content revealed that *amy3 bam1* mutant plants lost water more quickly than the wild type. After 1 h of stress, the water content in *amy3 bam1* had already decreased by 25% relative to the control, whereas the wild type only lost 7% of water (Figure 2A). Leaf sap osmolality increased in parallel with the loss of water, and by the end of the stress treatment, *amy3 bam1* showed an increase of 44% compared with a 29% increase in the wild type (Figure 2B). Furthermore, less water was absorbed and transpired by *amy3 bam1* under stress than by the wild type (only 63 and 79% as much after 2 and 3 h of mannitol treatment, respectively; Supplemental Figure 6). We recently reported that stomatal opening is impaired in *amy3 bam1* mutants due to the constitutive high levels of guard cell starch in these plants (Horrer et al., 2016). However, despite the differences in stomatal width (reduced in *amy3 bam1*), both the wild type and *amy3 bam1* closed their stomata at similar rates upon transfer to a mannitol-containing solution (Figure 2C). Thus, the rapid loss of water in *amy3 bam1* during the first hour of mannitol treatment cannot be explained by differences in stomatal closure. If transpiration through stomata were the main determinant of *amy3 bam1* responses to osmotic stress, a reduced rather than an increased loss of water would be expected. It is more likely that the reduced water absorption ability of *amy3 bam1* affected the water content in the leaves.

To assess the possibility that underground plant parts are involved in osmotic stress responses in *amy3 bam1*, we applied the stress to seedlings grown on half-strength Murashige and Skoog (MS) vertical agar plates. Six days (6 d) after germination, seedlings with the same root lengths were transferred for an additional 9 d to agar plates optionally supplemented with 300 mM mannitol. Primary root growth was reduced in the wild type upon stress. However, *amy3 bam1* showed a higher degree of inhibition (Figure 2D). Fresh weight measurements after 9 d of stress treatment showed that *amy3 bam1* and wild-type root growth was inhibited by 48 and 61%, respectively, relative to the controls (Figure 2E). Interestingly, shoot growth inhibition was similar for both genotypes (~63 to 66% of control; Figure 2E), resulting in substantial differences in root to shoot ratios. Wild-type plants increased their root to shoot ratio by 75% relative to the controls, whereas in *amy3 bam1*, the ratios remained unaltered (Figure 2F). Altogether, these results suggest that AMY3/BAM1-mediated leaf starch degradation contributes to osmotic stress tolerance by affecting root growth and function in response to stress.

Carbon Export to the Root and Osmolyte Accumulation during Osmotic Stress Are Reduced in *amy3 bam1*

The root phenotype of *amy3 bam1* suggests that stress-induced starch degradation affects the metabolism of the plant as whole. We therefore used $^{14}CO_2$ labeling to analyze carbon partitioning into different cellular compound classes and to measure carbon export from leaves to the roots in hydroponically grown plants with or without mannitol. We supplied $^{14}CO_2$ to the whole plant for 1 h, either at the beginning of the stress (after 3 h of light) or in the middle of the stress treatment (after 5 h of light). In each case, the $^{14}CO_2$ pulse was followed by 1 h chase in air (Figure 3A), after which the rosettes and roots were harvested separately. Under control conditions, carbon partitioning in wild-type and *amy3 bam1* plants was very similar (Supplemental Tables 1 and 2). Under osmotic stress, however, the two genotypes differed markedly in the amount of carbon channeled to the root. While the wild type maintained a high rate of carbon export during the whole experiment, *amy3 bam1* showed no increase in ^{14}C export after 4 h of stress (Figure 3B). Subfractionation of root-soluble compounds revealed that most of the imported carbon was present in neutral compounds (i.e., sugars), with no significant changes in the basic and acidic fractions (Figure 3C). Consistent with reduced carbon export to the root, the amount of label found in neutral sugars after 4 h of stress in *amy3 bam1* roots was reduced compared with the wild type (Figure 3C). Conversely, carbon allocation within the leaf soluble fraction was similar between the two genotypes, showing an increase in neutral sugars and a reduction in basic and acidic compounds (Figure 3D). This was accompanied by a decrease in carbon partitioning into starch and cell wall (Figure 3E). Interestingly, even though the labeling of starch and cell wall in *amy3 bam1* leaves after 4 h of stress was unchanged compared with the controls (Figure 3E), the amount of carbon allocation into leaf soluble sugars was still elevated relative to the unstressed control plants, as with the wild type (Figure 3E). This suggests that most of these sugars derive from photosynthetic carbon assimilation and only partly from starch hydrolysis. Alternatively, *amy3 bam1* might suffer from reduced sugar phloem loading.

Consistent with the ^{14}C-labeling experiments, we found that wild-type plants under osmotic stress accumulated much higher levels of soluble sugars, mostly sucrose, both in leaves and roots (Figures 4A to 4C; Supplemental Figures 7A to 7C). Proline also accumulated in high amounts toward the end of the stress treatment (Figure 4D; Supplemental Figure 7D). In *amy3 bam1* plants, the amount of soluble sugars and proline that accumulated in the root upon osmotic stress was reduced compared with the wild type (Figure 4), whereas sugar and proline accumulation in the leaves was only mildly impaired (Supplemental Figure 7).

Figure 1. (continued).

(B) and **(C)** Leaf starch **(B)** and maltose **(C)** content in osmotically stressed leaves compared with controls. Values are means ± SE ($n = 8$). FW, fresh weight.
(D) Leaf transcript abundance for *BAM1*, *BAM3*, and *AMY3* in osmotically stressed and control leaves, determined by qPCR. Plants grown as above were harvested at the indicated time points. The *ACT2* gene was used as a reference gene. *RD29A* was used as a positive stress-induced control. Values were normalized against gene expression at T0 (set as 1) and represent means ± SE ($n = 3$). Statistical significances determined by unpaired two-tailed Student's *t* tests: *P < 0.05 for the indicated comparison; #P < 0.05 mutants versus the wild type at the indicated time points; n.s., not significant for the indicated comparison.

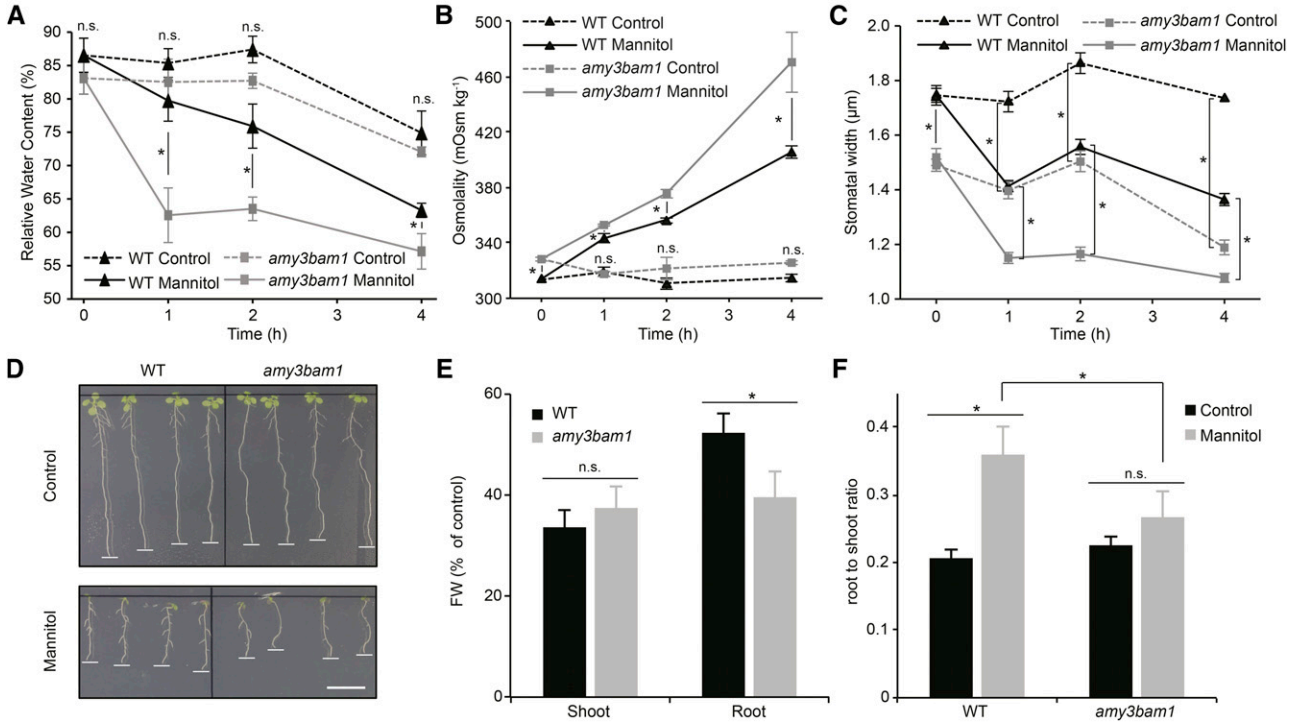

Figure 2. Effects of Osmotic Stress on *amy3 bam1* Double Mutants.

(A) Leaf relative water content of wild-type and *amy3 bam1* plants subject to mannitol stress or kept in control solution was determined at the indicated time points as described in Methods. Values are means ± SE (n = 6).

(B) Osmolality of wild-type and *amy3 bam1* leaf sap. Values are means ± SE (n = 6).

(C) Stomatal closure in response to mannitol treatment in wild type and *amy3 bam1* plants. Epidermal peels isolated from leaves of hydroponically grown plants treated with mannitol for 4 h or kept in a control nutrient solution were used for stomatal width measurements. Values are means ± SE (n = 4 biological replicates with more than 50 individual stomata measured for each time point).

(D) Morphology of wild-type and *amy3 bam1* plants under control (top panel) and osmotic stress conditions (bottom panel). Plants were grown in control medium for 6 d, transferred to medium optionally supplemented with 300 mM mannitol, and photographed 3 d later. Bar = 1 cm.

(E) Shoot and root fresh weights (FW) measured 9 d after seedling transfer as described in **(D)**. Values represent the FW of osmotically stressed plants compared with control plants (set as 100%). Values are means ± SE (n = 15).

(F) Root to shoot ratio of wild-type and *amy3 bam1* plants in response to 300 mM mannitol stress. Values are derived from the data shown in **(E)**. Statistical significances determined by unpaired two-tailed Student's t tests: *P < 0.05 for the indicated comparison; n.s., not significant for the indicated comparison.

Thus, osmotic stress seems to lead to (1) carbon accumulating in sugars, both in leaves and roots; (2) increased carbon export to the root; and (3) a reduction in carbon partitioning toward starch and cell wall. The most obvious consequence of defective starch degradation upon osmotic stress in the *amy3 bam1* mutant is a reduction in carbon allocation to the root, which may explain the hypersensitivity of *amy3 bam1* to the stress treatment.

Application of Exogenous ABA Induces *BAM1* and *AMY3* Expression and Results in Increased BAM1 Enzyme Activity and Starch Degradation

Mannitol treatment caused an increase in endogenous ABA levels in the leaves of both wild-type and *amy3 bam1* plants (Supplemental Figure 8). The rapid biosynthesis of ABA is recognized as one of the pivotal events in osmotic stress responses. ABA facilitates stomatal closure and induces the expression of many stress-responsive genes that protect plants from further water loss and damage (Urano et al., 2009; Yamaguchi-Shinozaki and Shinozaki, 2006; Choudhury and Lahiri, 2011; Böhmer and Schroeder, 2011; Zeller et al., 2009; Matsui et al., 2008; Kempa et al., 2008). We wondered whether ABA had an effect on leaf starch metabolism. Exogenously applied ABA (4 h) induced the expression of *BAM1*, *RD29A*, and, to a lesser extent, *AMY3* but had no effect on *BAM3* (Figure 5A), somewhat mirroring the behavior of these genes under osmotic stress treatment (Figure 1D). BAM1 levels and activity already increased in ABA-treated plants relative to untreated plants after 2 h of exposure to ABA (Figures 5B and 5C; Supplemental Figure 9), indicating that transcriptional activation resulted in rapid de novo protein synthesis. In contrast, there was no detectable change in AMY3 protein level in response to ABA (Supplemental Figure 5B). However, *AMY3* transcripts and spectra matching AMY3-derived peptides are frequently detected in many tissues types, especially leaves (Supplemental Figure 5A) (Baerenfaller et al., 2011), suggesting that the protein is already relatively abundant and that it most likely undergoes

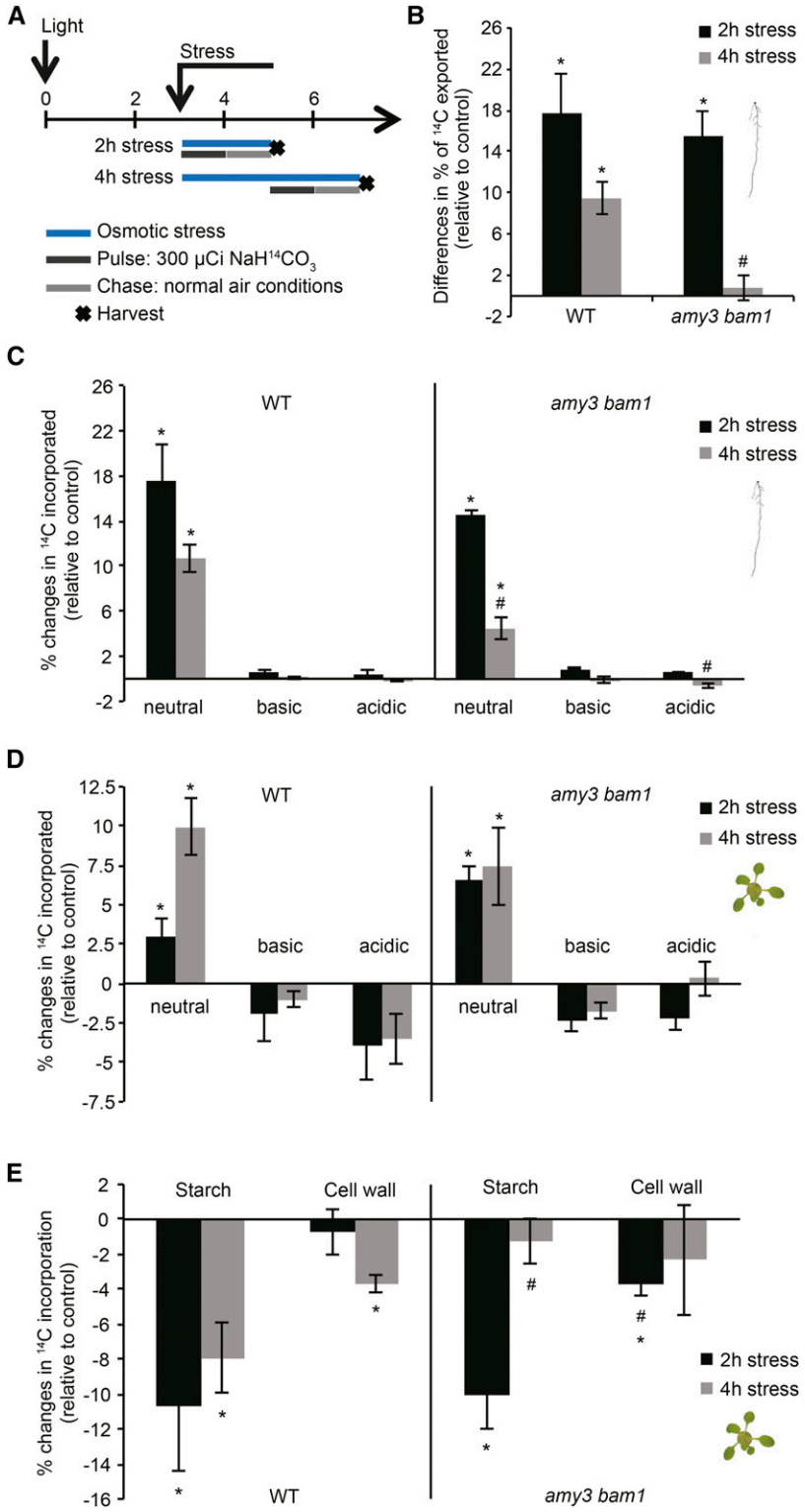

Figure 3. Carbon Partitioning in Wild-Type and *amy3 bam1* Plants during Osmotic Stress.

(A) Scheme of labeling set up. Whole wild-type and *amy3 bam1* plants were labeled with $^{14}CO_2$ for 1 h, just after transfer to a mannitol-containing nutrient solution or at the middle of the stress treatment. Following a 1-h chase period, the shoot and root were harvested separately and the ^{14}C in the different tissue fractions determined by scintillation counting.

posttranslational regulation. Interestingly, ABA-treated plants accumulated less starch than the controls, and maltose levels were high (Figures 5D and 5E). In contrast, ABA-sprayed *amy3 bam1* mutants accumulated similar amounts of starch to untreated plants, and maltose levels were slightly reduced, indicating that starch degradation in response to ABA was not activated in this mutant (Figures 5D and 5E). Despite the differences in stomatal width at the beginning of the ABA treatment (reduced in *amy3 bam1*, as expected), the wild type and *amy3 bam1* reduced their stomatal width to a similar extent (1.13 and 1.18 μm, respectively) within the first hour (Figure 5F). It is possible that during stomatal closure, ABA-regulated *AMY3* and *BAM1* expression might provide a feedback mechanism that controls stomatal width by increasing osmotically active solute concentrations, thereby counteracting the effects of potassium ion efflux. Stomata stayed closed in both genotypes until the end of the experiment (Figure 5F).

Altogether, these results suggest that exogenous ABA can trigger BAM1/AMY3-mediated starch degradation in the leaves and that this effect is independent of ABA-induced stomatal closure.

The ABA-Deficient Mutants *nced3* and *aba2* Mimic the *amy3 bam1* Phenotype under Osmotic Stress

An essential step in stress-induced de novo ABA biosynthesis is the cleavage of epoxycarotenoids to produce xanthoxin (the first C15 intermediate) by the 9-*cis* EPOXYCAROTENOID DIOXYGENASE3 (NCED3) (Iuchi et al., 2001). This explains why the *nced3*-null mutant does not accumulate ABA in response to dehydration (Iuchi et al., 2001; Urano et al., 2009). We used the *nced3* mutant to further investigate the role of ABA in stress-responsive starch metabolism. Under osmotic stress, *nced3* mimicked the behavior of *amy3 bam1*: Starch degradation was abolished and maltose levels remained unchanged compared with control plants, whereas the wild type activated starch degradation, as expected (Figures 6A and 6B). Given the tight link between ABA and sugar signaling pathways (reviewed in Hey et al., 2010), we wondered whether the defective starch degradation in *nced3* under osmotic stress was simply a secondary effect of ABA-sugar crosstalk rather than a direct consequence of the lack of stress-induced de novo ABA biosynthesis. We then investigated the phenotype of other ABA-related mutants. Similar to *nced3*, the ABA-deficient mutant *aba2* fails to synthesize ABA, as it lacks the short-chain alcohol dehydrogenase ABA2 responsible for the conversion of xanthoxin to abscisic aldehyde (González-Guzmán et al., 2002; Schwartz et al., 1997). As observed for *nced3*, *aba2* also failed to activate starch degradation and showed no or much reduced maltose accumulation in response to osmotic stress (Supplemental Figure 10). In contrast, the *aao3* mutant, lacking the ABSCISIC ALDEHYDE OXIDASE3 (AAO3) responsible for the final step in ABA biosynthesis (Seo and Koshiba, 2002), activated starch degradation similarly to the wild type (Figures 6A and 6B). Given that Arabidopsis contains four *AAO* genes with partially redundant functions (Seo et al., 2004), *aao3* mutants accumulate reduced but still detectable levels of ABA in response to dehydration stress (Seo et al., 2000), which may account for the activation of starch degradation in this mutant. Furthermore, *BAM1*, as well as *RD29A*, were significantly upregulated in response to stress in *aao3*, although to a lesser extent compared with the wild type, but were not induced in *nced3* (Figure 6C). *AMY3* was upregulated in the wild type, but not in *aao3* or *nced3* (Figure 6C), substantiating the importance of posttranslational regulation for the activation of AMY3 under stress. As expected, *BAM3* gene expression remained unaltered in all tested genotypes (Figure 6C). Together, these results show that the differences in ABA levels between the wild type and *aao3*, *nced3*, and *aba2* mutants are likely to be responsible for the observed differences in stress-induced starch degradation, suggesting that de novo ABA biosynthesis in response to osmotic stress is required for starch degradation. Consistently, exogenous application of ABA alone or in combination with mannitol restored starch degradation in the *nced3* mutant to almost wild-type levels (Supplemental Figure 11).

The AREB/ABF-SnRK2 Pathway Regulates ABA-Dependent *BAM1* and *AMY3* Gene Expression

To understand the molecular link between ABA and starch degradation during osmotic stress, we searched the promoter regions of *BAM1* and *AMY3* genes for known ABA-dependent *cis*-regulatory elements. Both *BAM1* and *AMY3* promoters contained ABA-responsive element (ABRE) motifs, while none were present in the *BAM3* promoter (Supplemental Data Set 1). The ABRE *cis*-regulatory elements are recognized by a group of bZIP transcription factors (TFs), the ABRE binding protein/ABRE binding factors (AREB/ABFs). These TFs have pivotal functions in ABA-dependent osmotic stress-responsive gene expression (Yoshida et al., 2010). In the presence of ABA, the AREB/ABF TFs are activated through phosphorylation by

Figure 3. (continued).

(B) Carbon export to the roots of osmotically stressed and control plants. Relative changes in ^{14}C imported into the root upon osmotic stress are given as percentages of that imported under control conditions (set as 0). Values are means ± SE ($n = 4$).

(C) Incorporation of ^{14}C into the different water-soluble fractions of wild-type and *amy3 bam1* roots. Relative changes in the amount of ^{14}C incorporated into the different fractions upon osmotic stress are given as percentages of that in corresponding fractions under control conditions (set as 0). Values are means ± SE ($n = 4$).

(D) Incorporation of ^{14}C into the different water-soluble fractions of wild-type and *amy3 bam1* shoots in plants subject to osmotic stress compared with controls. Relative changes are expressed as described above for **(C)**.

(E) Incorporation of ^{14}C into starch and cell wall compounds of wild-type and *amy3 bam1* shoots in plants subject to osmotic stress compared with control. Relative changes are expressed as described above for **(C)**. Statistical significances determined by unpaired two-tailed Student's *t* tests: *$P < 0.05$ for the indicated comparison; #$P < 0.05$ mutant versus the wild type at the indicated time points; n.s., not significant.

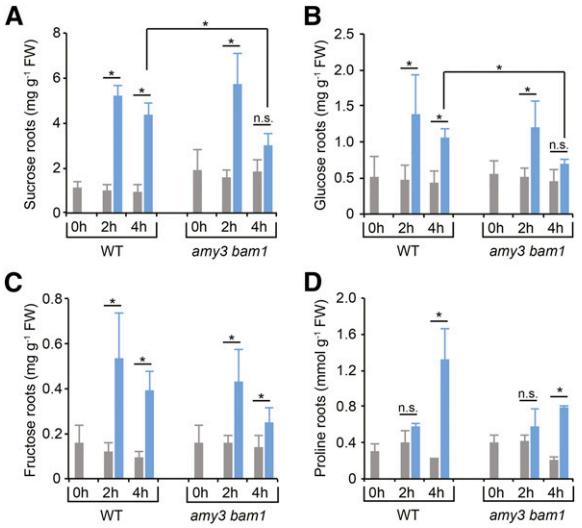

Figure 4. Quantification of Soluble Sugars and Proline in Roots of Osmotically Stressed Plants.

Sucrose **(A)**, glucose **(B)**, fructose **(C)**, and proline **(D)** content in roots of wild-type and *amy3 bam1* plants in response to osmotic stress treatment. Hydroponically grown plants were optionally supplemented with 300 mM mannitol for 4 h. Value are means ± SE ($n = 5$). FW, fresh weight. Statistical significances determined by unpaired two-tailed Student's *t* tests: *P < 0.05 for the indicated comparison; n.s., not significant for the indicated comparison.

SNF1-related kinase 2s (SnRK2s) (Fujita et al., 2009; Furihata et al., 2006), enabling them to bind the ABRE motifs in the promoters of the target genes, thereby activating their expression (Yoshida et al., 2014; Fujita et al., 2013).

The transcriptional activation of *BAM1* and *AMY3* in response to exogenously applied ABA was abolished in mutants lacking three SnRK2 kinases, *snrk2.2 snrk2.3 snrk2.6*, or greatly reduced in mutants lacking three AREB/ABF TFs, *areb1 areb2 abf3* (Figure 7A), all known positive regulators of ABA signaling in the leaves (Nakashima et al., 2009; Umezawa et al., 2009; Fujita et al., 2009; Fujii and Zhu, 2009; Yoshida et al., 2010). The residual transcriptional activation of *BAM1* in the *areb1 areb2 abf3* mutant was most likely due to the remaining activity of another bZIP TF, ABF1, which is also part of the AREB/ABF-Snrk2 signaling pathways in leaves under osmotic stress (Yoshida et al., 2015). Under control conditions, *BAM1* and *AMY3* transcript levels were similar to the wild type in both *snrk2.2 snrk2.3 snrk2.6* and *areb1 areb2 abf3* mutants (Supplemental Figure 12). *BAM3* transcript levels remained unaltered in response to ABA treatment in both mutants, similarly to the wild type (Figure 7A), consistent with the idea that BAM3 induction is not part of the ABA/osmotic stress responses. The *snrk2.2 snrk2.3 snrk2.6* mutant showed a severe wilting phenotype (Fujii and Zhu, 2009), which prevented its successful cultivation in hydroponics. We therefore used the *areb1 areb2 abf3* mutant for further experiments and found that BAM1 protein levels did not change in response to exogenous application of ABA (Figures 7B and 7C), and starch degradation upon mannitol treatment was significantly reduced compared with the wild type (Figures 7D and 7E). Collectively, these findings suggest that ABA-dependent SnRK2 signaling mediates BAM1 and AMY3 activation in response to osmotic stress through AREB1, AREB2, ABF3, and, possibly, ABF1 TFs.

ABREs Are Conserved in the Promoters of *BAM1* Orthologs

In Arabidopsis, the presence of ABREs in the *BAM1* promoter clearly distinguishes BAM1 from BAM3. To determine if this is a general feature of β-amylases from flowering plants, we scanned the promoters of *BAM1* and *BAM3* orthologs from 30 different angiosperm species for the presence of conserved sequence motifs, using the MEME algorithm (Bailey et al., 2009). MEME revealed a collection of conserved motifs across the *BAM1* ortholog promoters, the most highly represented of which was only found in the Eudicots and had a sequence logo CACGTGTC, with a highly significant E-value of 3.6e-49 (Figure 8A; Supplemental Data Set 1). This sequence almost precisely matched the ABRE motif (PyACGTGG/TC) (Zhang et al., 2005; Gómez-Porras et al., 2007), indicating that ABRE *cis*-acting elements are conserved in *BAM1* orthologs from all the eudicotyledon species analyzed here. The distance of the ABREs to the translational start codon (ATG) was also conserved. They were mostly found in the proximity of the ATG in the interval 100 to 400 bp (Figure 8B), consistent with the occurrence of ABREs previously reported for the Arabidopsis genome (Gómez-Porras et al., 2007).

A second motif conserved in all of the analyzed BAM1 orthologs promoters had the sequence logo CA/GCCG/AT/CCC (Figure 8C; Supplemental Data Set 1), which resembled a coupling element 3 (CE3)-like motif (Zhang et al., 2005; Gómez-Porras et al., 2007). CE3-like motifs are found in the promoters of many ABA-responsive genes, often coupled to ABREs. A combination of ABRE/CE3-like motifs was initially thought to establish a minimal ABA-responsive complex to confer ABA responsiveness (Shen and Ho, 1995; Shen et al., 1996). In fact, it was later shown that the ACGT-containing ABREs and CE3 are functionally equivalent *cis*-acting elements and that multiple ABREs or CEs or the combination of ABREs with CEs can also confer ABA responsiveness (Hobo et al., 1999). In our analysis, it is interesting that while ABREs elements were practically absent in the promoters of *BAM1* orthologs from monocotyledons, the CE3-like motifs were universally present (Figure 8B). It is possible that BAM1 orthologs from monocotyledons can be induced by ABA in the absence of ABRE elements, for example, through multiple CE motifs. This hypothesis is consistent with a recent study showing that in rice (*Oryza sativa*), CE3 motifs are overrepresented and ~80 times more frequent than in Arabidopsis (Gómez-Porras et al., 2007). In the promoters of *BAM3* orthologs genes, the MEME algorithm retrieved conserved sequences which could not be assigned to any known regulatory motif (Supplemental Data Set 1). Altogether, this analysis suggests that the presence of ABA responsive elements is a conserved feature of *BAM1* orthologs genes.

DISCUSSION

A Critical Role for Starch Degradation in Osmotic Stress Tolerance

Crops and other plants in natural conditions are routinely affected by a broad range of abiotic and biotic stresses acting simultaneously or in sequence. This results in a high degree of complexity

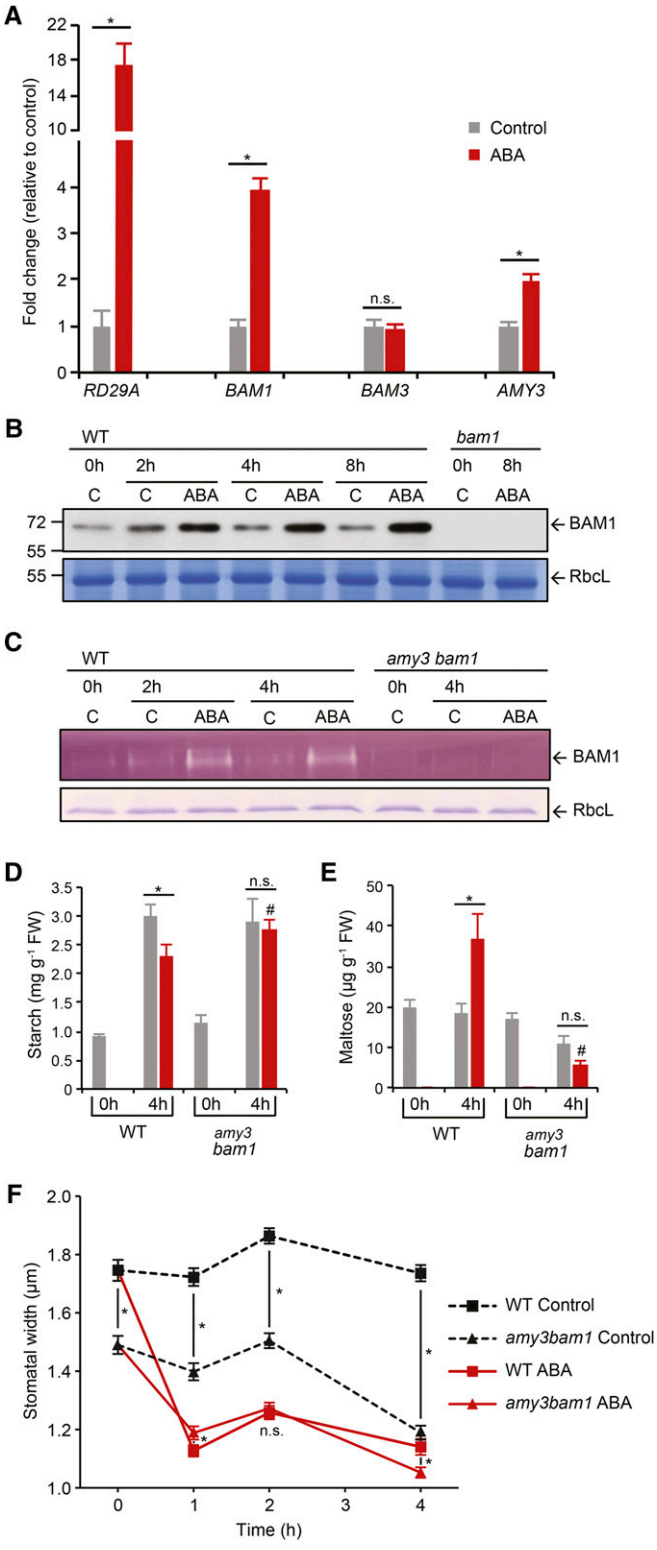

Figure 5. Effects of Exogenous ABA on Leaf Starch Metabolism.

(A) Relative expression levels of *BAM1*, *BAM3*, and *AMY3* in wild type leaves 4 h after treatment with 100 µM ABA, determined by qPCR. The *ACT2* gene served as a reference gene. *RD29A* served as a positive control for the ABA treatment. Values representing means ± SE ($n = 3$) were normalized against gene expression in control conditions (set as 1).

(B) Immunodetection of BAM1 protein in wild-type leaves after ABA treatment. Total protein was extracted from rosettes of hydroponically grown plants at the indicated time points. Equal protein amounts were separated by SDS-PAGE. The Rubisco large subunit (RbcL), the dominant band visualized by Coomassie staining, confirmed uniform loading. BAM1 was detected using polyclonal antibodies raised against recombinant BAM1. Extracts of the *bam1* mutant served as a negative control. Replicate blots yielded the same result. C, mock-treated control.

(C) ABA-mediated changes in BAM1 activity. Leaf crude extracts from hydroponically grown wild-type and *amy3 bam1* plants harvested 4 h after ABA treatment were separated by native PAGE in gels containing 0.1% amylopectin. After electrophoresis and incubation for 2 h (see Methods), the gels were stained in Lugol's solution. BAM1 activity was detected in wild-type but not *amy3 bam1* plants.

(D) and **(E)** Leaf starch **(D)** and maltose **(E)** content in wild-type and *amy3 bam1* plants 4 h after ABA treatment, compared with controls. Values are means ± SE ($n = 6$). FW, fresh weight.

(F) Stomatal closure in response to ABA treatment in wild-type and *amy3 bam1* plants. Epidermal peels isolated from leaves of hydroponically grown plants treated with ABA 100 µM for 4 h or kept in a control nutrient solution were used for stomatal width measurements. Values are means ± SE ($n = 4$ biological replicates with more than 50 individual stomata measured for each time point). Stomatal width under control conditions is the same as in Figure 2C, as the experiments were conducted in parallel. Statistical significances determined by unpaired two-tailed Student's *t* tests: *$P < 0.05$ for the indicated comparison; #$P < 0.05$ mutant versus the wild type at the indicated time points; n.s., not significant for the indicated comparison.

in plant stress responses in the field, making it often difficult to dissect the single components. In this study, the use of hydroponic and agar plate systems enabled us to investigate the effects of osmotic stress on both leaves and roots and define the role of stress-induced starch degradation on the metabolism of the plant as a whole. Even though the field environment is very different from the controlled conditions used in the laboratory, our discovery uncovers a critical function for starch in plant osmotic stress tolerance and highlights two starch hydrolases, AMY3 and BAM1, as targets for future studies under field conditions.

We provide evidence that the reduction in starch accumulation in Arabidopsis plants exposed to a short-term, high osmotic stress is, at least in part, a result of induced starch degradation, leading to the production of maltose, the major starch catabolite (Figures 1B and 1C). In mutants lacking AMY3 and BAM1, this metabolic stress response was abolished and starch accumulation was the same as in control conditions (Figures 1B and 1C). Furthermore, the maltose levels in the starch-less Arabidopsis mutant *pgm* remained unchanged in response to osmotic stress (Supplemental Figure 2). Concomitantly with the induction of starch degradation, wild-type plants responded to the osmotic stress by accumulating high levels of sugars and proline in the leaves (Supplemental Figure 7), presumably for osmotic adjustment and energy supply to maintain cell survival and metabolic activity (Couée et al., 2006; Verslues and Sharma, 2011). Our data suggest that most of these osmolytes derived from photosynthetic carbon assimilation and only partly from starch hydrolysis. First, *amy3 bam1* plants were only mildly impaired in leaf sugar accumulation during stress and showed no differences from the

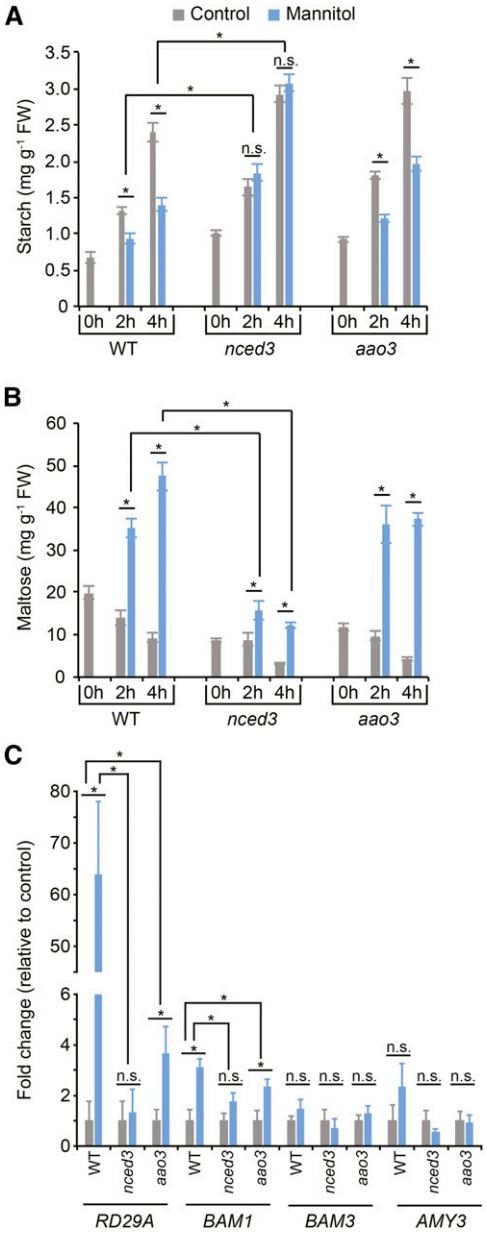

Figure 6. Leaf Starch Degradation during Osmotic Stress Is Blocked in the ABA-Deficient Mutant *nced3*.

(A) and **(B)** Leaf starch **(A)** and maltose **(B)** content in wild-type, *nced3*, and *aao3* plants treated with 300 mM mannitol compared with controls. Values are means ± SE (n = 6). FW, fresh weight.

(C) Relative expression levels of *BAM1*, *BAM3*, and *AMY3* in leaves of wild-type, *nced3*, and *aao3* plants treated with 300 mM mannitol for 4 h, determined by qPCR. The *ACT2* gene served as a reference gene. *RD29A* served as a positive control for the osmotic stress treatment. Values representing means ± SE (n = 3) were normalized against gene expression in control conditions (set as 1). Statistical significances determined by unpaired two-tailed Student's t tests: *P < 0.05 for the indicated comparison; n.s., not significant for the indicated comparison.

wild type in leaf proline accumulation (Supplemental Figure 7). Moreover, our ^{14}C labeling experiments showed that carbon partitioning into the leaf soluble neutral fraction during stress was similar in wild-type and *amy3 bam1* plants (Figure 3D). Consistent with this, we observed that osmotic stress caused only a transient decrease in the PSII operating efficiency (ΦPSII), which was similar in the two genotypes (Supplemental Table 3) and, importantly, did not hinder the capacity of the plants to assimilate $^{14}CO_2$. However, sugars may also accumulate in leaves because of decreased demand, as a consequence of shoot growth limitation (Hummel et al., 2010), or because of decreased starch biosynthesis (Geigenberger et al., 1997). This might be caused by changes in phosphorylated intermediates, especially 3-phosphoglycerate, reduction of which would inactivate ADP-glucose pyrophosphorylase, the regulated enzyme of starch biosynthesis (Heldt et al., 1977). A decline in 3-phosphoglycerate under stress could result from impaired photosynthesis (Kaplan and Guy, 2005; Scarpeci and Valle, 2008) or from the activation of the sucrose biosynthesis in response to stress through sucrose synthase phosphate (Geigenberger et al., 1997), which would compete for assimilates. It was indeed demonstrated that phosphorylation of sucrose synthase phosphate is a mechanism for osmotic stress activation of this enzyme in spinach leaves (Toroser and Huber, 1997).

Major differences between the wild type and *amy3 bam1* were apparent in the amount of carbon channeled to the root under osmotic stress. This was markedly reduced in the mutant compared with the wild type, especially after 4 h of mannitol treatment (Figure 3B). Consequently, *amy3 bam1* had reduced levels of sugars and proline in the roots (Figure 4). It is possible that starch degradation in the leaves is required to increase carbon exported to the roots during osmotic stress (Figure 9). However, it cannot be excluded that *amy3 bam1* suffered additional defects, such as impaired phloem loading and long distance sugar transport, which would contribute to the complexity of the observed phenotype. Reduced carbon export in *amy3 bam1* most likely affected the ability of the root to absorb water and nutrients from the medium (Supplemental Figure 6; Figure 9). An early study reported that inorganic ion uptake regulates turgor in osmotically stressed Arabidopsis epidermal root cells (Shabala and Lew, 2002). Thus, carbon export to the root during osmotic stress could provide the energy needed for this uptake, besides directly contributing to the root osmotic adjustment.

There was also an impact on root growth. While wild-type plants responded to osmotic stress by increasing their root to shoot ratio, the ratio in *amy3 bam1* remained unchanged compared with non-stress conditions (Figure 2F). Adjustment of root growth under stress is an important survival strategy, allowing plants to expand the root (at the expense of shoot growth) to increase nutrient and water uptake capacity (Wu and Cosgrove, 2000; Rogers and Benfey, 2015; Roycewicz and Malamy, 2012). Our results are consistent with these observations and reveal a function of starch degradation in controlling root growth in response to osmotic stress (Figure 9).

Differential Regulation and Isoform Subfunctionalization Define the Adaptive Plasticity of Plant Starch Metabolism

The two close homologs, BAM1 and BAM3, are differentially regulated in response to abiotic stresses (Figure 1D; Supplemental Figure 13) (Maruyama et al., 2009; Kaplan and Guy, 2004; Monroe

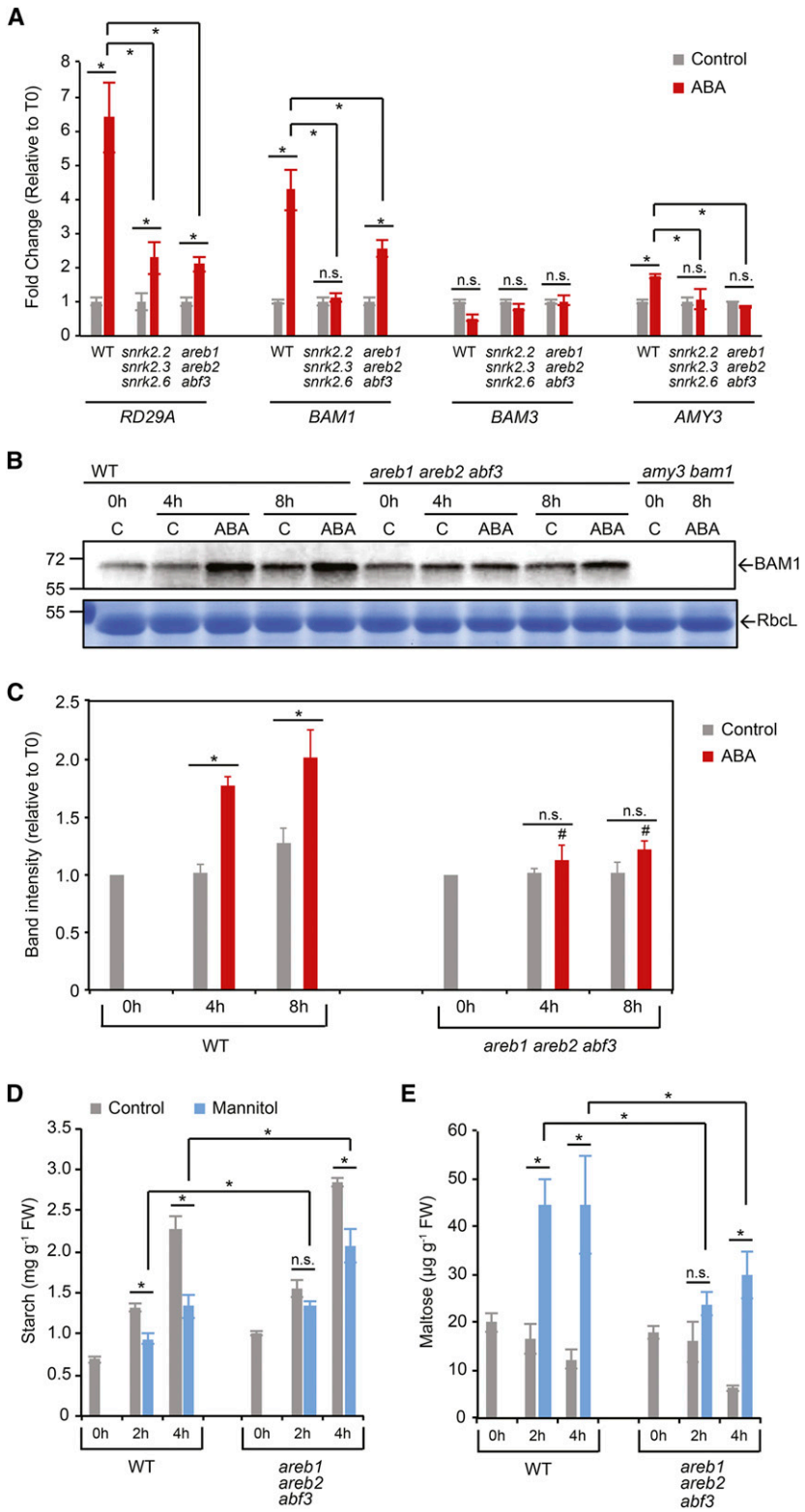

Figure 7. AREB1, AREB2, and ABF3 Transcription Factors Regulate *BAM1* and *AMY3* Expression in Response to Osmotic Stress.

(A) Relative expression levels of *BAM1*, *BAM3*, and *AMY3* in the wild type and *areb1 areb2 abf3* triple mutant leaves 4 h after treatment with 100 µM ABA, determined by qPCR. The *ACT2* gene served as a reference gene. *RD29A* served as a positive control for the ABA treatment. Values representing means ± SE (n = 3) were normalized against gene expression in control conditions (set as 1).

(B) Immunodetection of BAM1 protein in wild-type, *areb1 areb2 abf3*, and *amy3 bam1* leaves after ABA treatment. Total protein was extracted from rosettes of hydroponically grown plants at the indicated time points. Equal amounts of protein were separated by SDS-PAGE and the Rubisco large subunit (RbcL)

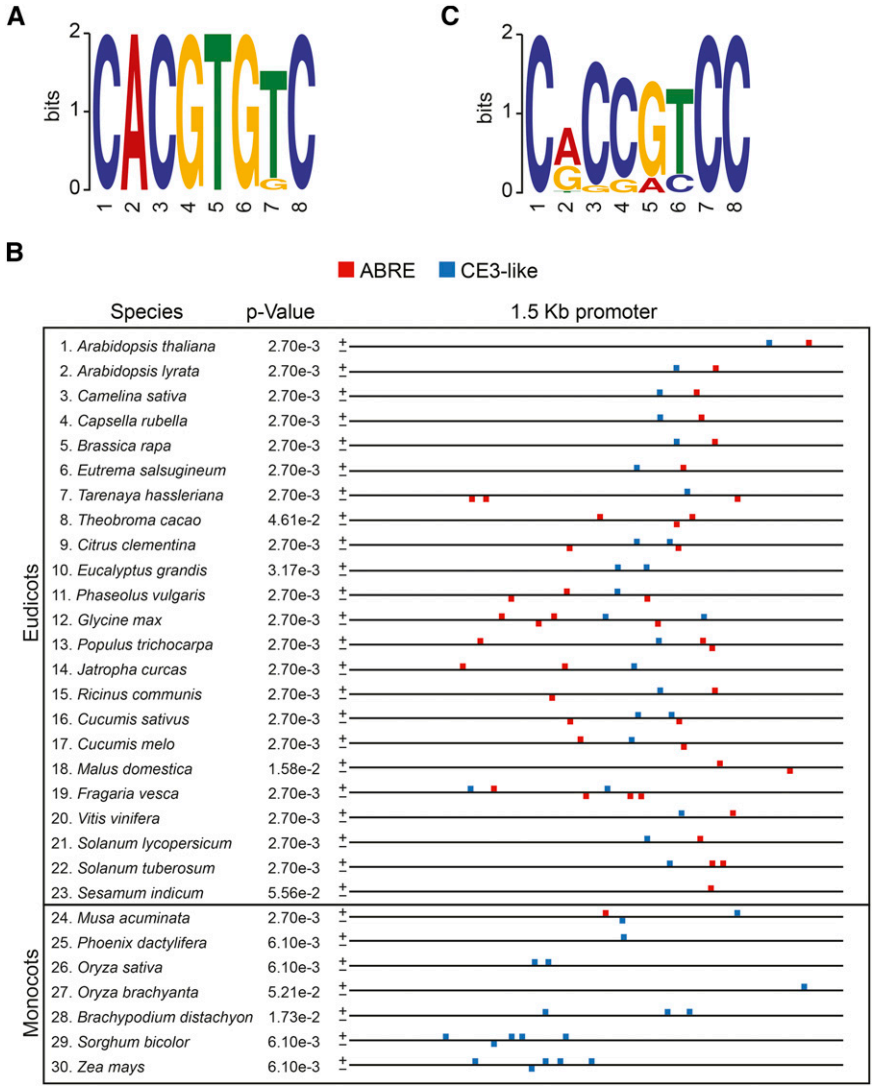

Figure 8. Unbiased Bioinformatics Analysis of *BAM1* Ortholog Promoter Sequences.

(A) and **(B)** The 1.5-kb promoter regions of *BAM1-like* genes from 30 angiosperm species were analyzed using the MEME algorithm (http://meme.nbcr.net). The conserved sequence logos of the ABREs and CE3-like found by MEME are depicted in **(A)** and **(B)**, respectively. The diagram provides an idea of which positions in the motif are most highly conserved (measured in bits). Highly conserved positions in the motif have higher bits.
(C) Distribution of ABRE and CE3-like *cis*-regulatory elements within the analyzed promoters.

et al., 2014). *BAM3* gene expression is induced by cold stress, whereas *BAM1* expression is induced by heat and by osmotic stress. The most obvious interpretation of this differential transcriptional regulation is that starch degradation can be induced by different signals. Mutant studies substantiate the hypothesis that *BAM1* induction is critically important in the osmotic stress response. As first reported by Valerio et al. (2011), we also found that *bam1* mutants had reduced starch degradation in response to

Figure 7. (continued).

was used for confirmation. BAM1 was detected using polyclonal antibody raised against recombinant BAM1. Replicate blots yielded the same result. C, control.
(C) BAM1 protein quantification. Densitometry analysis (ImageJ) was used to quantify band intensities such as in **(B)**. Values are means ± SE of three biological samples, each analyzed with three technical replicates, and expressed relative to the mean band intensity at time 0 (T0, set as 1).
(D) and **(E)** Starch **(D)** and maltose **(E)** content in wild-type and *areb1 areb2 abf3* plants subject to mannitol stress compared with controls. Values are means ± SE ($n = 6$). FW, fresh weight. Statistical significances determined by unpaired two-tailed Student's *t* tests: *P < 0.05 for the indicated comparison; #P < 0.05 mutant versus the wild type at the indicated time points; n.s., not significant for the indicated comparison.

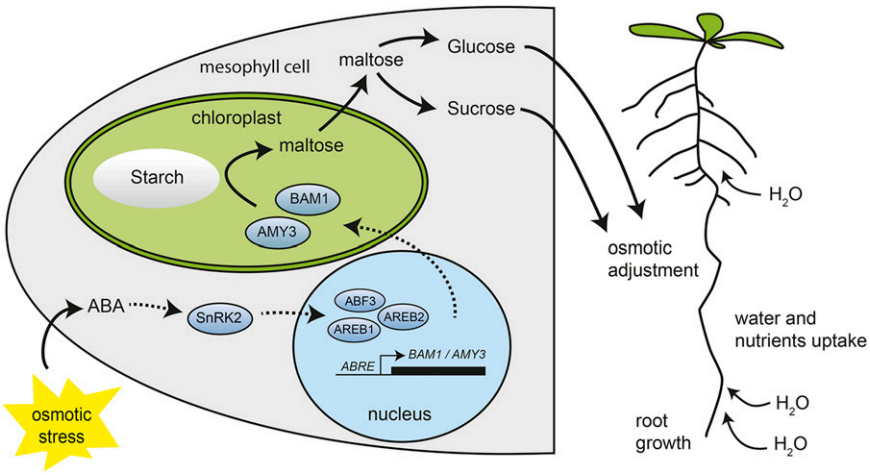

Figure 9. Proposed Model of Starch Degradation Mechanism and Regulation during Osmotic Stress.

In response to stress, ABA triggers *BAM1* and *AMY3* transcription through the ABA-dependent AREB/ABF-SnRK2 signaling pathway. This leads to rapid de novo BAM1 protein synthesis and increased amylolytic activity, although posttranslational modifications are also likely to contribute. A fraction of the maltose released from starch by the synergistic action of BAM1 and AMY3 is exported to the cytosol and metabolized into sucrose and free hexoses. Sucrose is then exported to the root to support osmotic adjustment, water and nutrient uptake, and root growth. The remaining sugars, including some maltose and the additional sugars originating from carbon assimilation, are retained in the leaves for osmotic adjustment, energy supply, and to protect the photosynthetic apparatus from oxidative stress.

short-term mannitol treatment (Figures 1B and 1C). In contrast, *bam3* mutants, though compromised in normal nighttime starch degradation (Supplemental Figure 3), could activate *BAM1* expression and starch degradation under osmotic stress conditions (Figures 1B and 1C; Supplemental Figure 4), showing that BAM3 is not part of the osmotic stressed-induced starch degradation pathway. A similar situation was found in guard cells. Under standard growth conditions, *BAM1* is preferentially and highly expressed in guard cells, whereas *BAM3* is considerably less abundant (Horrer et al., 2016). Consistent with the gene expression pattern, *bam1* mutants have elevated guard cell starch levels compared with the wild type, whereas *bam3* accumulates starch in this cell type similarly to the wild type (Horrer et al., 2016; Valerio et al., 2011). Altogether, these findings indicate that BAM1 and BAM3 are active under different conditions and in a cell type-specific manner. Subfunctionalization among members of the β-amylase family has occurred that significantly contributed to the ability of the plant to adjust starch turnover to the need of the individual cells and in response to the external environmental stimuli (Monroe et al., 2014; Zanella et al., 2016; Horrer et al., 2016).

Besides subfunctionalization, synergy among the enzymes of starch degradation is also critical in defining starch adaptive plasticity. We recently showed that BAM1 and AMY3 work synergistically in guard cells to degrade starch during stomatal opening (Horrer et al., 2016). Here, we report that AMY3 is also involved with BAM1 in mediating starch breakdown in the leaves in response to osmotic stress. It is conspicuous that the loss of both enzymes does not affect starch metabolism under normal conditions (Supplemental Figure 3), yet completely blocks starch degradation in guard cells (Horrer et al., 2016) or in the leaves upon osmotic stress (Figures 1B and 1C). These contrasting phenotypes hint at an intricate network of differential regulation which defines subfunctionalization among the enzymes of starch degradation, with some required for the mobilization of starch to respond to stress, and others required for normal nighttime starch degradation in leaves or for daytime starch degradation in guard cells.

Previous work suggests that it may not be just the gene expression patterns, but also the characteristics of encoded BAM1 and AMY3 enzymes themselves, that distinguish them from other starch-degrading enzymes and make them suitable for starch degradation during daytime. For example, both enzymes are redox regulated, whereby they can be rapidly activated through reduction via the light-driven ferredoxin-thioredoxin system (Sparla et al., 2006; Seung et al., 2013). Furthermore, both enzymes are preferentially active at a slightly alkaline pH (Seung et al., 2013; Sparla et al., 2006; Monroe et al., 2014; Santelia et al., 2015). Thus, the reducing environment and the alkaline pH of the stroma, generated by the photosynthetic electron transport chain in the light (Heldt et al., 1973; Buchanan and Balmer, 2005), would favor BAM1 and AMY3 activity. Conversely, there is no evidence for redox regulation of BAM3, and the enzyme has optimum activity at less alkaline pH (Santelia et al., 2015; Monroe et al., 2014). Furthermore, large-scale site-specific phosphorylation profiling of Arabidopsis proteins revealed the presence of one or more phosphorylation sites on both BAM1 and AMY3 proteins (de la Fuente van Bentem et al., 2008; Reiland et al., 2009; Xue et al., 2013; Heazlewood et al., 2008). Given the rapid activation of leaf starch degradation in response to the osmotic stress, it is likely that posttranslational modifications such as protein phosphorylation or redox regulation played a major role in activating BAM1 and AMY3 in the light. This would be particularly crucial for AMY3, as the protein was already relative abundant in the leaves, and no changes in protein levels were detected upon treatment (Supplemental Figure 5).

Lastly, it should be noted that there are likely to be factors required for starch degradation in osmotic stress conditions other than BAM1 and AMY3. For example, the enzymes mediating the phosphorylation and dephosphorylation of starch, a process that precedes its degradation by amylases, may be required for osmotic stress-induced degradation as well as for normal nighttime degradation (Yano et al., 2005; Silver et al., 2014; Kötting et al., 2010). However, GWD, which phosphorylates the C6-position of glucosyl residues (Ritte et al., 2006), was reported to be involved in the cold-induced development of freezing tolerance (Yano et al., 2005), similar to BAM3 (Kaplan and Guy, 2004). Thus, it is plausible that a certain degree of subfunctionalization also exists within the enzymes of glucan phosphorylation, with GWD required for the mobilization of starch under cold stress, and PWD, which phosphorylates the C3 positions, required for the activation of starch degradation under osmotic stress.

ABA Is the Primary Signal for Starch Degradation in Leaves in Response to Osmotic Stress

One of the pivotal events in osmotic stress responses is the rapid, transient accumulation of ABA, which facilitates stomatal closure and expression of ABA-responsive genes that protect plants from further water loss and damage. Several transcriptomic analyses have reported ABA-dependent induction of a multitude of dehydration stress-related genes, as well as some involved in primary carbohydrate metabolism (Böhmer and Schroeder, 2011; Kempa et al., 2008; Matsui et al., 2008; Choudhury and Lahiri, 2011; Urano et al., 2009; Fujita et al., 2011). Here, we showed that BAM1 and AMY3 are targets of the ABA/osmotic-dependent AREB/ABF-SnRK2 pathway and that ABA is required for osmotic stress-induced starch degradation in the leaves (Figure 9). Exogenously applied ABA induced *BAM1* and *AMY3* expression in the wild type, but not in mutants lacking key components of the leaf ABA/osmotic-dependent signaling pathway (Figure 7A) (Yoshida et al., 2014; Fujii and Zhu, 2009). Consistently, exogenously applied ABA stimulated starch degradation in the wild type, but not in the double mutant *amy3 bam1* (Figures 5D and 5E), and this effect appeared to be independent of ABA-induced stomatal closure (Figure 5F). Thus, activation of BAM1 and AMY3 in response to ABA (Figures 5B and 5C; Supplemental Figure 5) induces starch degradation. Lastly, osmotic stress-induced starch degradation was abolished in the *nced3* and *aba2* mutants, but not in a mutant lacking AAO3 (Figures 6A and 6B; Supplemental Figure 10). Given that the major difference between these ABA biosynthetic mutants is their capacity to accumulate ABA in response to stress (Seo et al., 2000; Iuchi et al., 2001; Urano et al., 2009), our data suggest that the lack of stress-induced starch degradation in *nced3* and *aba2* was specifically caused by the complete absence of ABA accumulation. This is supported by the observation that the stress-induced transcriptional induction of *BAM1* and *AMY3* was substantially impaired in *nced3*, but not in *aao3* (Figure 6C). These observations are in line with previous transcriptomic and metabolic data and lead to the conclusion that de novo biosynthesis of ABA is the trigger for starch degradation in the light in response to osmotic stress.

Both *BAM1* and *AMY3* promoters contain ABRE motifs, which are absent in the *BAM3* promoter (Supplemental Data Set 1), consistent with the observation that *BAM3* is not ABA-induced. Pairs of BAM1 and BAM3 orthologs are found in the genomes of several angiosperms, suggesting that BAM isoform subfunctionalization is a general feature of flowering plants (Monroe et al., 2014; Fulton et al., 2008). Interestingly, bioinformatics analyses of the promoters of *BAM1* and *BAM3* orthologs from 30 different plant species using the MEME algorithm (Bailey et al., 2009) revealed an enrichment of ABRE elements in the proximity of the ATG codon in all examined *BAM1-like* gene promoters, with the exception of that of the grasses, where instead CE3-like ABA-responsive elements were found (Figure 8; Supplemental Data Set 1). Furthermore, ABRE or CE3 were absent in all examined *BAM3-like* gene promoters (Supplemental Data Set 1). This suggests that the presence of ABA-responsive elements is a conserved feature of *BAM1* orthologs and that the regulation of starch degradation by ABA during stress through the AREB/ABF-SnRK2 pathway is most likely a conserved mechanism across many plant species.

METHODS

Plant Materials and Growth Conditions

The following *Arabidopsis thaliana* T-DNA insertion mutants were used in this study: *bam1* (Salk_039895), *bam3* (CS92461) (Fulton et al., 2008), *amy3-2* (Sail_613 D12) (Yu et al., 2005), *amy3 bam1* (Horrer et al., 2016), *snrk2.2 snrk2.3 snrk2.6* (Fujii and Zhu, 2009), *areb1 areb2 abf3* (Yoshida et al., 2010), *aao3-4* (Salk_072361) (Seo et al., 2004), *nced3* (GABI_129B08) (Wan and Li, 2006), and *aba2-1* (G1464A) (Léon-Kloosterziel et al., 1996). Arabidopsis ecotype Columbia-0 (Col-0) was used as the wild type in all experiments.

Plants were grown in soil or in hydroponic culture as previously described (Kölling et al., 2015) in a controlled environment chamber (KKD Hiross, CLITEC Boulaguiem) in a 12-h-light/12-h-dark cycle with a constant temperature of 23°C, 45% relative humidity, and a uniform illumination of 120 μmol m^{-2} s^{-1} (Osram L36W/965 Biolux and Osram L36/W77 Biolux at 3:1 ratio; continuous spectra). To induce osmotic stress, 3-week-old hydroponically grown plants were transferred to a nutrient solution supplemented with 300 mM mannitol or 300 mM sorbitol for 4 h, starting after 3 h of light. The rosettes and the roots were harvested separately at the indicated time points for further analyses. As a control, a subset of plants were kept in a nutrient solution without osmotic agents and harvested at the same time points. Alternatively, sterilized seeds were germinated on half-strength MS vertical plates, containing 0.8% (w/v) agar. Six days after germination, seedlings with the same root length were transferred for additional 9 d to MS plates optionally supplemented with 300 mM mannitol. Primary roots were measured using the ImageJ plug-in NeuronJ (Meijering et al., 2004) to determine growth rates. For ABA treatment, 3-week-old hydroponically grown plants were sprayed with 100 μM ABA-KOH in 0.01% (v/v) Tween 20, or a mock solution, starting after 3 h of light, and rosettes were harvested at different time points for further analyses.

qPCR Analysis of Transcript Levels

Total RNA was extracted from leaves using an RNeasy Plant Mini Kit (Qiagen) according to the manufacturer's instructions. Following DNase-I treatment, 1 μg of total RNA of each sample was used to produce cDNA using the M-MLV reverse transcriptase and oligo(dT) primers (Promega). Quantitative PCR was performed using SYBR green master mix with the 7500 Fast Real-Time PCR System (Applied Biosystems). Reactions were run in triplicate with three different cDNA preparations, and the instrument's iQ5 Optical System Software was used to determine the threshold cycle (Ct). Gene-specific transcripts were normalized to the *Actin2* gene (*ACT2*; At3g18780) and quantified by the ΔCt method (Ct of gene of interest – Ct of *ACT2* gene). Real-time SYBR green dissociation curves showed one species of amplicon for each primer combination listed in Supplemental Table 4.

Iodine Staining

Four-week-old Arabidopsis rosettes were harvested at the end of day or end of night and incubated in 80% (v/v) ethanol for 12 h to remove the chlorophyll. The cleared plants were rinsed in water and stained in Lugol's solution (Sigma-Aldrich) for 10 min.

Quantification of Starch and Leaf Soluble Sugars

Rosettes from plants grown in hydroponic culture or in soil were harvested into liquid N_2 and extracted in 0.7 M perchloric acid as previously described (Hostettler et al., 2011). Starch in the insoluble fraction was determined by measuring the amount of glucose released by treatment with α-amylase and amyloglucosidase (both from Roche). Sugars (maltose, glucose, fructose, and sucrose) in the soluble fraction were determined using HPAEC-PAD (Dionex ICS-5000; Thermo Scientific). Samples of the neutralized soluble fraction (200 μL) were applied to sequential 1.5-mL columns of cation exchanger Dowex 50 W and anion exchanger Dowex 1 (Sigma-Aldrich). Neutral compounds were eluted with 5 mL of water, lyophilized, redissolved in 200 μL of water, and separated on a CarboPac PA20 column on an ICS-3000 system (Dionex) as previously described (Egli et al., 2010). Peaks were identified by coelution with known malto-oligosaccharide standards and areas were determined using the instrument's Chromeleon software.

Quantification of Root Soluble Sugars

Root sugar measurements were performed on 3-week-old hydroponically grown plants optionally supplemented with 300 mM mannitol for 2 or 4 h. At the indicated time points, roots from three plants were harvested and pooled, rinsed briefly with deionized water to remove residual mannitol, weighed, and snap frozen in liquid N_2. Roots were pulverized while still frozen using the Mix Mill MM-301 (Retsch) and extracted in 1 mL 80% (v/v) ethanol for 15 min at 80°C. The pellet was sequentially washed with 0.5 mL 50% (v/v) ethanol, 20% (v/v) ethanol, and deionized water. The supernatants from each wash were pooled, dried under vacuum, and resuspended in 200 μL of water. Glucose, fructose, and sucrose were quantified enzymatically by adapting an existing method (Viola and Davies, 1992). Briefly, 15 μL of samples were added to 183 mL of 50 mM HEPES buffer, pH 7.5, containing 1 mM ATP, 1 mM NAD, and 1 mM $MgCl_2$. To measure glucose, hexokinase (Roche) and glucose 6-phosphate dehydrogenase (Roche) were used to convert glucose to 6-phosphogluconate with concomitant reduction of NAD to NADH, which was monitored spectrophotometrically at 340 nm. Subsequently, phosphoglucoisomerase (Roche) was added to determine the amount of fructose. Finally, invertase (Sigma-Aldrich) was added to cleave sucrose into fructose and glucose. The further increase in OD_{340} represented sucrose.

$^{14}CO_2$ Pulse-Chase Labeling

Whole-plant labeling experiments were performed with 3-week-old hydroponically grown plants optionally supplemented with 300 mM mannitol for 2 or 4 h. Plants were labeled as previously described (Kölling et al., 2015) using a sealed Plexiglas chamber illuminated with 120 μmol m^{-2} s^{-1}. $^{14}CO_2$ (300 μCi) was supplied for 60 min, either at the beginning of the stress (after 3 h of light) or in the middle of the stress treatment (after 5 h of light), after which the Plexiglas chamber was opened and the plants were kept in normal air for a chase period of 60 min (see Figure 3A for a schematic representation of the labeling set up). After the chase, the rosettes and the roots were harvested separately, the different tissues was fractionated between water soluble (neutral, acidic, and basic), ethanol soluble, and insoluble (starch and cell wall) compounds and the ^{14}C determined as described previously (Kölling et al., 2013).

Proline Quantification

Free proline content of rosettes and roots of hydroponically grown plants under control conditions or subject to mannitol stress was measured by adaptation of an existing method (Bates et al., 1973). In short, 200 μL of the soluble fraction from the sugar measurements were mixed with 800 μL of water, 1 mL of glacial acetic acid, and 1 mL of ninhydrin reagent (2.5% ninhydrin in a 6:3:1 mixture of glacial acetic acid:water:orthophosphoric acid). Samples were incubated for 1 h at 90°C, cooled to 25°C, combined with an equal volume of toluene, and mixed vigorously. Following phase partitioning, 1 mL of the upper organic phase was transferred into a quartz cuvette and the OD at 546 nm was measured spectrophotometrically. A calibration curve was prepared using different proline concentrations as a standard.

Measurements of Endogenous ABA Levels

Endogenous ABA content was measured in leaves of hydroponically grown plants with or without mannitol treatment for 4 h. Samples were extracted and measured as described in (Großkinsky et al., 2014).

Relative Water Content

Relative water content was measured in leaves of 3-week-old hydroponically grown plants with or without mannitol treatment and used as a measure of water loss in response to the stress. Rosettes were weighed at the time of sampling (fresh weight) and after incubation in deionized water for 24 h (rehydrated weight). Dry weight after 24 h at 50°C was also measured. Plant water status was evaluated from the relative water content [(fresh weight − dry weight)/(rehydrated weight − dry weight) * 100].

Osmolality (π)

For osmolyte concentration measurements, leaves from three plants were pooled, subject to five cycles of freezing/thawing, and subsequently mechanically ground. After centrifugation for 10 min at 16,000*g* at 4°C, 10 μL of the diluted supernatant (generally 1:3) was used to determine the osmolality using a Micro-Osmometer (Advance Instruments).

Determination of F_v/F_m and ΦPSII

Chlorophyll fluorescence transients of Col-0 and *amy3 bam1* leaves in response to osmotic stress were measured using the FluorCam 800MF (Photo Systems Instruments). The fluorescence measurement protocol uses short (30 μs) measuring flashes to measure the initial minimal fluorescence (F_o) emitted from dark-adapted leaves, followed by a strong saturating flash for 0.8 s measure the maximal fluorescence (F_m). After 15 min of dark adaptation, the leaf was exposed to actinic light for 4 min. Three strong flashes of saturating light probed the effective quantum yield (ΦPSII) during the actinic light exposure. The chlorophyll fluorescence transients were measured at the indicated time points in plants subject to 300 mM mannitol stress or kept in control nutrient solution. Image processing software integrated with the FluorCam (www.psi.cz) was used to process the captured time-resolved ChlF images. The numeric value of each ChlF parameter was determined by integrating it over the measured leaf area using the following formula: $F_v/F_m = (F_m - F_o)/F_m$; $\Phi PSII = F_m' - F'/F_m'$, where F_m' is the maximal fluorescence from light-adapted leaves and F' is the fluorescence emission from light-adapted leaves.

Stomatal Width

For stomatal width measurement, epidermal peels isolated from the abaxial side of the middle part of leaf 6 were glued onto a cover slip using a nontoxic medical adhesive (Medical Adhesive B Liquid, VM 355-1, Ulrich Swiss). The adaxial epidermis and mesophyll layers were gently removed. The cover slips with the glued abaxial epidermis were rinsed with 10 mM MES-KOH, pH 6.15, and stomata were immediately imaged using an inverted microscope (Nikon Eclipse TS100) at 40× magnification. Stomatal width was measured manually using ImageJ software (v 1.42q, NIH USA; http://

rsbweb.nih.gov/ij/). Around 20 pictures per leaf and per time point were taken, and more than 50 stomatal widths were measured.

Native PAGE and Activity Staining

Entire rosettes of hydroponically grown culture were harvested at the indicated time points and frozen in liquid N_2. Rosettes were ground using the Mix Mill MM-301 (Retsch) and incubated for 30 min at 4°C in extraction buffer (50 mM Tris-HCl, pH 7.5, 1 mM $CaCl_2$, 1 mM $MgCl_2$, 5 mM DTT, and 1× Complete EDTA Free Protease Inhibitor [Roche]; 300 μL per 100 mg fresh weight) for 30 min at 4°C. Insoluble material was removed by centrifugation at 15,000*g* for 5 min. Protein content was quantified using the BCA Protein Assay kit (Thermo Scientific), and 5 μg of protein was loaded onto the PAGE gels. For native PAGE, resolving gels contained 7.5% (w/v) acrylamide, 9% (v/v) glycerol, 375 mM Tris-HCl, pH 8.8, and 0.1% (w/v) amylopectin. The stacking gel contained 3.75% (w/v) acrylamide, 63 mM Tris-HCl, pH 6.8, and 0.1% (w/v) amylopectin. Protein extracts from leaves were mixed with PAGE loading buffer (final concentration 50 mM Tris-HCl, pH 6.8, 3% [v/v] glycerol, and 0.005% [w/v] bromophenol blue) and loaded onto the gel (5 μg protein). After 3 h electrophoresis at 4°C with a constant 120 V, the gels were washed once in a reducing incubation buffer (100 mM HEPES-KOH, pH 7.5, 1 mM $CaCl_2$, 1 mM $MgCl_2$, and 5 mM DTT) and then incubated for 2 h in the same buffer at 25°C. The gels were stained for 16 h at 4°C in Lugol's solution. Excess stain was removed by several washes in cold water.

Immunodetection of BAM1 and AMY3 Protein and Quantification

Rosettes of control and ABA-treated plants were harvested into microcentrifuge tubes containing three glass beads and kept frozen at −80°C prior to analysis. The tissue was ground into a fine powder using a Mix Mill. Protein extraction medium (40 mM Tris-HCl, pH 6.8, 5 mM $MgCl_2$, and Protease inhibitor cocktail [Roche]) was added to the powder at a ratio of 1 mL per 100 mg tissue. Insoluble material was spun down at 20,000*g* for 5 min, and soluble proteins were collected in the supernatant. Protein (5 μg) was loaded onto SDS-PAGE gels and electrophoresis performed using standard protocols. For immunoblotting, proteins were transferred onto a PVDF membrane following SDS-PAGE. The BAM1 protein was detected using a polyclonal rabbit antibody (Eurogentec) raised against a recombinant His-tagged Arabidopsis BAM1 protein, which was expressed and purified from *Escherichia coli*. Antibodies specific for BAM1 were affinity purified from the antiserum against the recombinant BAM1 protein conjugated to NHS-activated Sepharose (GE healthcare). The purified antibody was used at a dilution of 1:10,000. AMY3 was detected using polyclonal antibodies raised against recombinant AMY3 protein (Yu et al., 2005), at a dilution of 1:3000. Bands were visualized by chemiluminescence detection. Quantification of band intensities was conducted using the densitometry feature of ImageJ software.

Accession Numbers

Sequence data from this article can be found in the GenBank/EMBL libraries under accession numbers: *ACT2* (At3g18780), *RD29A*, (At5g52310), *BAM1* (At3g23920), *AMY3* (At1g69830), *BAM3* (At4g17090), *PGM* (At5g51820), *NCED3* (At3g14440), *ABA2* (At1g52340), *AAO3* (At2g27150), *AREB1* (At1g45249), *AREB2* (At3g19290), *ABF1* (At1g49720), *ABF3* (At4g34000), *SNRK2.2* (At3g50500), *SNRK2.3* (At5g66880), and *SNRK2.6* (At4g33950).

Supplemental Data

Supplemental Figure 1. Starch and maltose levels in wild-type plants upon mannitol or sorbitol treatment.

Supplemental Figure 2. Starch and maltose levels in wild-type and *pgm* mutant plants upon mannitol treatment.

Supplemental Figure 3. Impact of simultaneous loss of BAM1 and AMY3 on starch metabolism in plants grown under control conditions.

Supplemental Figure 4. Expression levels of *BAM1* in wild-type and *bam3* mutant plants.

Supplemental Figure 5. AMY3 is a highly abundant protein in plant leaves.

Supplemental Figure 6. Water absorption by wild-type and *amy3 bam1* plants in response to mannitol stress.

Supplemental Figure 7. Soluble sugars and proline content of shoots in response to osmotic stress.

Supplemental Figure 8. Accumulation of endogenous ABA in response to mannitol treatment.

Supplemental Figure 9. Quantification of BAM1 protein in leaves of wild-type plants treated with ABA.

Supplemental Figure 10. Starch and maltose levels in wild-type and *aba2* mutant plants upon mannitol treatment.

Supplemental Figure 11. Starch levels in response to mannitol, ABA, or a combination of mannitol and ABA treatment.

Supplemental Figure 12. Expression levels of *RD29A*, *BAM1*, *BAM3*, and *AMY3* in *snrk2.2 snrk2.3 snrk2.6* and *areb1 areb2 abf3* mutants under control conditions.

Supplemental Figure 13. *BAM1* and *BAM3* are differentially regulated by abiotic stresses.

Supplemental Table 1. Carbon partitioning into the major cellular compound classes in shoots and roots of plants labeled at the beginning of the stress treatment.

Supplemental Table 2. Carbon partitioning into the major cellular compound classes in shoots and roots of plants labeled in the middle of the stress treatment.

Supplemental Table 3. Chlorophyll *a* fluorescence parameters of wild-type and *amy3 bam1* plants subject to osmotic stress.

Supplemental Table 4. Sequences of primers used in this work.

Supplemental Data Set 1. Promoter sequences used for the MEME analysis in Figure 8.

ACKNOWLEDGMENTS

We thank Michaela Stettler for technical help with the ^{14}C labeling experiments and the HPAEC-PAD analysis; Martina Zanella for support with the free proline measurements; Mario Coiro for support with the MEME analysis; Jan-Kang Zhu for providing the *snrk2.2 snrk2.3 snrk2.6* mutant; Kazuko Yamaguchi-Shinozaki for providing the *areb1 areb2 abf3* mutant; Florian Bittner for providing *aao3-4* and *aba2-1* mutants; and Enrico Martinoia, Stefan Hörtensteiner, and Luis Lopez Molina for helpful discussion. This work was supported by the Swiss National Science Foundation SNSF-Grant 31003A_147074 (to D. Santelia), by the Forschungskredit_13-101 from the University of Zürich (to M.T.), by a Heinz-Imhof Fellowship from the ETH Foundation (to D. Seung), and by the SystemsX.ch RTD project "Plant growth in a changing environment" and the EU FP7 project TiMet, Grant 245143 (to S.C.Z.).

AUTHOR CONTRIBUTIONS

D. Santelia conceived the project. D. Santelia and M.T. designed the experiments. D. Santelia, M.T., D.P., D. Seung, D.H., A.N., T.M., K.K.,

and H.W.P. performed the experiments and analyzed the data. D. Santelia, M.T., and S.C.Z. wrote the article.

Received February 22, 2016; revised July 5, 2016; accepted July 19, 2016; published July 19, 2016.

REFERENCES

Baerenfaller, K., Hirsch-Hoffmann, M., Svozil, J., Hull, R., Russenberger, D., Bischof, S., Lu, Q., Gruissem, W., and Baginsky, S. (2011). pep2pro: a new tool for comprehensive proteome data analysis to reveal information about organ-specific proteomes in *Arabidopsis thaliana*. Integr. Biol. (Camb.) **3:** 225–237.

Bailey, T.L., Boden, M., Buske, F.A., Frith, M., Grant, C.E., Clementi, L., Ren, J., Li, W.W., and Noble, W.S. (2009). MEME SUITE: tools for motif discovery and searching. Nucleic Acids Res. **37:** W202–W208.

Bartels, D., and Sunkar, R. (2005). Drought and salt tolerance in plants. CRC. Crit. Rev. Plant Sci. **24:** 23–58.

Bates, L.S., Waldren, R.P., and Teare, I.D. (1973). Rapid determination of free proline for water-stress studies. Plant Soil **39:** 205–207.

Blatt, M.R. (2016). Plant physiology: redefining the enigma of metabolism in stomatal movement. Curr. Biol. **26:** R107–R109.

Böhmer, M., and Schroeder, J.I. (2011). Quantitative transcriptomic analysis of abscisic acid-induced and reactive oxygen species-dependent expression changes and proteomic profiling in Arabidopsis suspension cells. Plant J. **67:** 105–118.

Buchanan, B.B., and Balmer, Y. (2005). Redox regulation: a broadening horizon. Annu. Rev. Plant Biol. **56:** 187–220.

Caspar, T., Huber, S.C., and Somerville, C. (1985). Alterations in growth, photosynthesis, and respiration in a starchless mutant of *Arabidopsis thaliana* (L.) deficient in chloroplast phosphoglucomutase activity. Plant Physiol. **79:** 11–17.

Choudhury, A., and Lahiri, A. (2011). Comparative analysis of abscisic acid-regulated transcriptomes in Arabidopsis. Plant Biol (Stuttg) **13:** 28–35.

Couée, I., Sulmon, C., Gouesbet, G., and El Amrani, A. (2006). Involvement of soluble sugars in reactive oxygen species balance and responses to oxidative stress in plants. J. Exp. Bot. **57:** 449–459.

de la Fuente van Bentem, S., et al. (2008). Site-specific phosphorylation profiling of Arabidopsis proteins by mass spectrometry and peptide chip analysis. J. Proteome Res. **7:** 2458–2470.

Edner, C., Li, J., Albrecht, T., Mahlow, S., Hejazi, M., Hussain, H., Kaplan, F., Guy, C., Smith, S.M., Steup, M., and Ritte, G. (2007). Glucan, water dikinase activity stimulates breakdown of starch granules by plastidial beta-amylases. Plant Physiol. **145:** 17–28.

Egli, B., Kölling, K., Köhler, C., Zeeman, S.C., and Streb, S. (2010). Loss of cytosolic phosphoglucomutase compromises gametophyte development in Arabidopsis. Plant Physiol. **154:** 1659–1671.

Fujii, H., and Zhu, J.-K. (2009). Arabidopsis mutant deficient in 3 abscisic acid-activated protein kinases reveals critical roles in growth, reproduction, and stress. Proc. Natl. Acad. Sci. USA **106:** 8380–8385.

Fujita, Y., et al. (2009). Three SnRK2 protein kinases are the main positive regulators of abscisic acid signaling in response to water stress in Arabidopsis. Plant Cell Physiol. **50:** 2123–2132.

Fujita, Y., Fujita, M., Shinozaki, K., and Yamaguchi-Shinozaki, K. (2011). ABA-mediated transcriptional regulation in response to osmotic stress in plants. J. Plant Res. **124:** 509–525.

Fujita, Y., Yoshida, T., and Yamaguchi-Shinozaki, K. (2013). Pivotal role of the AREB/ABF-SnRK2 pathway in ABRE-mediated transcription in response to osmotic stress in plants. Physiol. Plant. **147:** 15–27.

Fulton, D.C., et al. (2008). Beta-AMYLASE4, a noncatalytic protein required for starch breakdown, acts upstream of three active beta-amylases in Arabidopsis chloroplasts. Plant Cell **20:** 1040–1058.

Furihata, T., Maruyama, K., Fujita, Y., Umezawa, T., Yoshida, R., Shinozaki, K., and Yamaguchi-Shinozaki, K. (2006). Abscisic acid-dependent multisite phosphorylation regulates the activity of a transcription activator AREB1. Proc. Natl. Acad. Sci. USA **103:** 1988–1993.

Geigenberger, P., Reimholz, R., Geiger, M., Merlo, L., Canale, V., and Stitt, M. (1997). Regulation of sucrose and starch metabolism in potato tubers in response to short-term water deficit. Planta **201:** 502–518.

Gibon, Y., Blaesing, O.E., Hannemann, J., Carillo, P., Höhne, M., Hendriks, J.H., Palacios, N., Cross, J., Selbig, J., and Stitt, M. (2004). A Robot-based platform to measure multiple enzyme activities in Arabidopsis using a set of cycling assays: comparison of changes of enzyme activities and transcript levels during diurnal cycles and in prolonged darkness. Plant Cell **16:** 3304–3325.

Gómez-Porras, J.L., Riaño-Pachón, D.M., Dreyer, I., Mayer, J.E., and Mueller-Roeber, B. (2007). Genome-wide analysis of ABA-responsive elements ABRE and CE3 reveals divergent patterns in Arabidopsis and rice. BMC Genomics **8:** 260.

González-Guzmán, M., Apostolova, N., Bellés, J.M., Barrero, J.M., Piqueras, P., Ponce, M.R., Micol, J.L., Serrano, R., and Rodríguez, P.L. (2002). The short-chain alcohol dehydrogenase ABA2 catalyzes the conversion of xanthoxin to abscisic aldehyde. Plant Cell **14:** 1833–1846.

Graf, A., Schlereth, A., Stitt, M., and Smith, A.M. (2010). Circadian control of carbohydrate availability for growth in Arabidopsis plants at night. Proc. Natl. Acad. Sci. USA **107:** 9458–9463.

Graf, A., and Smith, A.M. (2011). Starch and the clock: the dark side of plant productivity. Trends Plant Sci. **16:** 169–175.

Großkinsky, D.K., Albacete, A., Jammer, A., Krbez, P., van der Graaff, E., Pfeifhofer, H., and Roitsch, T. (2014). A rapid phytohormone and phytoalexin screening method for physiological phenotyping. Mol. Plant **7:** 1053–1056.

Heazlewood, J.L., Durek, P., Hummel, J., Selbig, J., Weckwerth, W., Walther, D., and Schulze, W.X. (2008). PhosPhAt: a database of phosphorylation sites in *Arabidopsis thaliana* and a plant-specific phosphorylation site predictor. Nucleic Acids Res. **36:** D1015–D1021.

Heldt, H.W., Chon, C.J., and Maronde, D. (1977). Role of orthophosphate and other factors in the regulation of starch formation in leaves and isolated chloroplasts. Plant Physiol. **59:** 1146–1155.

Heldt, W.H., Werdan, K., Milovancev, M., and Geller, G. (1973). Alkalization of the chloroplast stroma caused by light-dependent proton flux into the thylakoid space. Biochim. Biophys. Acta **314:** 224–241.

Hey, S.J., Byrne, E., and Halford, N.G. (2010). The interface between metabolic and stress signalling. Ann. Bot. (Lond.) **105:** 197–203.

Hobo, T., Asada, M., Kowyama, Y., and Hattori, T. (1999). ACGT-containing abscisic acid response element (ABRE) and coupling element 3 (CE3) are functionally equivalent. Plant J. **19:** 679–689.

Hoekstra, F.A., Golovina, E.A., and Buitink, J. (2001). Mechanisms of plant desiccation tolerance. Trends Plant Sci. **6:** 431–438.

Horrer, D., Flütsch, S., Pazmino, D., Matthews, J.S.A., Thalmann, M., Nigro, A., Leonhardt, N., Lawson, T., and Santelia, D. (2016). Blue light induces a distinct starch degradation pathway in guard cells for stomatal opening. Curr. Biol. **26:** 362–370.

Hostettler, C., Kölling, K., Santelia, D., Streb, S., Kötting, O., and Zeeman, S.C. (2011). Analysis of starch metabolism in chloroplasts. Methods Mol. Biol. **775:** 387–410.

Hummel, I., Pantin, F., Sulpice, R., Piques, M., Rolland, G., Dauzat, M., Christophe, A., Pervent, M., Bouteillé, M., Stitt, M., Gibon, Y., and Muller, B. (2010). Arabidopsis plants acclimate to water deficit

at low cost through changes of carbon usage: an integrated perspective using growth, metabolite, enzyme, and gene expression analysis. Plant Physiol. **154:** 357–372.

Iuchi, S., Kobayashi, M., Taji, T., Naramoto, M., Seki, M., Kato, T., Tabata, S., Kakubari, Y., Yamaguchi-Shinozaki, K., and Shinozaki, K. (2001). Regulation of drought tolerance by gene manipulation of 9-cis-epoxycarotenoid dioxygenase, a key enzyme in abscisic acid biosynthesis in Arabidopsis. Plant J. **27:** 325–333.

Kaplan, F., and Guy, C.L. (2004). beta-Amylase induction and the protective role of maltose during temperature shock. Plant Physiol. **135:** 1674–1684.

Kaplan, F., and Guy, C.L. (2005). RNA interference of Arabidopsis beta-amylase8 prevents maltose accumulation upon cold shock and increases sensitivity of PSII photochemical efficiency to freezing stress. Plant J. **44:** 730–743.

Kaplan, F., Kopka, J., Sung, D.Y., Zhao, W., Popp, M., Porat, R., and Guy, C.L. (2007). Transcript and metabolite profiling during cold acclimation of Arabidopsis reveals an intricate relationship of cold-regulated gene expression with modifications in metabolite content. Plant J. **50:** 967–981.

Kempa, S., Krasensky, J., Dal Santo, S., Kopka, J., and Jonak, C. (2008). A central role of abscisic acid in stress-regulated carbohydrate metabolism. PLoS One **3:** e3935.

Kölling, K., Müller, A., Flütsch, P., and Zeeman, S.C. (2013). A device for single leaf labelling with CO_2 isotopes to study carbon allocation and partitioning in *Arabidopsis thaliana.* Plant Methods **9:** 45.

Kölling, K., Thalmann, M., Müller, A., Jenny, C., and Zeeman, S.C. (2015). Carbon partitioning in *Arabidopsis thaliana* is a dynamic process controlled by the plants metabolic status and its circadian clock. Plant Cell Environ. **38:** 1965–1979.

Kötting, O., Kossmann, J., Zeeman, S.C., and Lloyd, J.R. (2010). Regulation of starch metabolism: the age of enlightenment? Curr. Opin. Plant Biol. **13:** 321–329.

Kötting, O., Santelia, D., Edner, C., Eicke, S., Marthaler, T., Gentry, M.S., Comparot-Moss, S., Chen, J., Smith, A.M., Steup, M., Ritte, G., and Zeeman, S.C. (2009). STARCH-EXCESS4 is a laforin-like Phosphoglucan phosphatase required for starch degradation in *Arabidopsis thaliana.* Plant Cell **21:** 334–346.

Krasensky, J., and Jonak, C. (2012). Drought, salt, and temperature stress-induced metabolic rearrangements and regulatory networks. J. Exp. Bot. **63:** 1593–1608.

Léon-Kloosterziel, K.M., Gil, M.A., Ruijs, G.J., Jacobsen, S.E., Olszewski, N.E., Schwartz, S.H., Zeevaart, J.A., and Koornneef, M. (1996). Isolation and characterization of abscisic acid-deficient Arabidopsis mutants at two new loci. Plant J. **10:** 655–661.

Lu, Y., Gehan, J.P., and Sharkey, T.D. (2005). Daylength and circadian effects on starch degradation and maltose metabolism. Plant Physiol. **138:** 2280–2291.

Maruyama, K., et al. (2009). Metabolic pathways involved in cold acclimation identified by integrated analysis of metabolites and transcripts regulated by DREB1A and DREB2A. Plant Physiol. **150:** 1972–1980.

Matsui, A., et al. (2008). Arabidopsis transcriptome analysis under drought, cold, high-salinity and ABA treatment conditions using a tiling array. Plant Cell Physiol. **49:** 1135–1149.

Meijering, E., Jacob, M., Sarria, J.-C.F., Steiner, P., Hirling, H., and Unser, M. (2004). Design and validation of a tool for neurite tracing and analysis in fluorescence microscopy images. Cytometry A **58:** 167–176.

Miller, G., Suzuki, N., Ciftci-Yilmaz, S., and Mittler, R. (2010). Reactive oxygen species homeostasis and signalling during drought and salinity stresses. Plant Cell Environ. **33:** 453–467.

Monroe, J.D., Storm, A.R., Badley, E.M., Lehman, M.D., Platt, S.M., Saunders, L.K., Schmitz, J.M., and Torres, C.E. (2014). β-Amylase1 and β-amylase3 are plastidic starch hydrolases in Arabidopsis that seem to be adapted for different thermal, pH, and stress conditions. Plant Physiol. **166:** 1748–1763.

Nakashima, K., Fujita, Y., Kanamori, N., Katagiri, T., Umezawa, T., Kidokoro, S., Maruyama, K., Yoshida, T., Ishiyama, K., Kobayashi, M., Shinozaki, K., and Yamaguchi-Shinozaki, K. (2009). Three Arabidopsis SnRK2 protein kinases, SRK2D/SnRK2.2, SRK2E/SnRK2.6/OST1 and SRK2I/SnRK2.3, involved in ABA signaling are essential for the control of seed development and dormancy. Plant Cell Physiol. **50:** 1345–1363.

Purdy, S.J., Bussell, J.D., Nunn, C.P., and Smith, S.M. (2013). Leaves of the Arabidopsis maltose exporter1 mutant exhibit a metabolic profile with features of cold acclimation in the warm. PLoS One **8:** e79412.

Reiland, S., Messerli, G., Baerenfaller, K., Gerrits, B., Endler, A., Grossmann, J., Gruissem, W., and Baginsky, S. (2009). Large-scale Arabidopsis phosphoproteome profiling reveals novel chloroplast kinase substrates and phosphorylation networks. Plant Physiol. **150:** 889–903.

Ritte, G., Heydenreich, M., Mahlow, S., Haebel, S., Kötting, O., and Steup, M. (2006). Phosphorylation of C6- and C3-positions of glucosyl residues in starch is catalysed by distinct dikinases. FEBS Lett. **580:** 4872–4876.

Rogers, E.D., and Benfey, P.N. (2015). Regulation of plant root system architecture: implications for crop advancement. Curr. Opin. Biotechnol. **32:** 93–98.

Roycewicz, P., and Malamy, J.E. (2012). Dissecting the effects of nitrate, sucrose and osmotic potential on Arabidopsis root and shoot system growth in laboratory assays. Philos. Trans. R. Soc. B Biol. Sci. **367:** 1489–1500.

Santelia, D., Trost, P., and Sparla, F. (2015). New insights into redox control of starch degradation. Curr. Opin. Plant Biol. **25:** 1–9.

Scarpeci, T.E., and Valle, E.M. (2008). Rearrangement of carbon metabolism in *Arabidopsis thaliana* subjected to oxidative stress condition: an emergency survival strategy. Plant Growth Regul. **54:** 133–142.

Schwartz, S.H., Léon-Kloosterziel, K.M., Koornneef, M., and Zeevaart, J.A. (1997). Biochemical characterization of the *aba2* and *aba3* mutants in *Arabidopsis thaliana*. Plant Physiol. **114:** 161–166.

Scialdone, A., and Howard, M. (2015). How plants manage food reserves at night: quantitative models and open questions. Front. Plant Sci. **6:** 204.

Seo, M., Aoki, H., Koiwai, H., Kamiya, Y., Nambara, E., and Koshiba, T. (2004). Comparative studies on the Arabidopsis aldehyde oxidase (AAO) gene family revealed a major role of AAO3 in ABA biosynthesis in seeds. Plant Cell Physiol. **45:** 1694–1703.

Seo, M., and Koshiba, T. (2002). Complex regulation of ABA biosynthesis in plants. Trends Plant Sci. **7:** 41–48.

Seo, M., Peeters, A.J., Koiwai, H., Oritani, T., Marion-Poll, A., Zeevaart, J.A., Koornneef, M., Kamiya, Y., and Koshiba, T. (2000). The Arabidopsis aldehyde oxidase 3 (AAO3) gene product catalyzes the final step in abscisic acid biosynthesis in leaves. Proc. Natl. Acad. Sci. USA **97:** 12908–12913.

Seung, D., Thalmann, M., Sparla, F., Abou Hachem, M., Lee, S.K., Issakidis-Bourguet, E., Svensson, B., Zeeman, S.C., and Santelia, D. (2013). *Arabidopsis thaliana* AMY3 is a unique redox-regulated chloroplastic α-amylase. J. Biol. Chem. **288:** 33620–33633.

Shabala, S.N., and Lew, R.R. (2002). Turgor regulation in osmotically stressed Arabidopsis epidermal root cells. Direct support for the role of inorganic ion uptake as revealed by concurrent flux and cell turgor measurements. Plant Physiol. **129:** 290–299.

Shen, Q., and Ho, T.H. (1995). Functional dissection of an abscisic acid (ABA)-inducible gene reveals two independent ABA-responsive complexes each containing a G-box and a novel cis-acting element. Plant Cell **7:** 295–307.

Shen, Q., Zhang, P., and Ho, T.H.D. (1996). Modular nature of abscisic acid (ABA) response complexes: composite promoter units that are necessary and sufficient for ABA induction of gene expression in barley. Plant Cell **8:** 1107–1119.

Silver, D.M., Kötting, O., and Moorhead, G.B.G. (2014). Phosphoglucan phosphatase function sheds light on starch degradation. Trends Plant Sci. **19:** 471–478.

Sitnicka, D., and Orzechowski, S. (2014). Cold-induced starch degradation in potato leaves — intercultivar differences in the gene expression and activity of key enzymes. Biol. Plant. **58:** 659–666.

Smith, A.M., and Stitt, M. (2007). Coordination of carbon supply and plant growth. Plant Cell Environ. **30:** 1126–1149.

Smith, S.M., Fulton, D.C., Chia, T., Thorneycroft, D., Chapple, A., Dunstan, H., Hylton, C., Zeeman, S.C., and Smith, A.M. (2004). Diurnal changes in the transcriptome encoding enzymes of starch metabolism provide evidence for both transcriptional and post-transcriptional regulation of starch metabolism in Arabidopsis leaves. Plant Physiol. **136:** 2687–2699.

Sparla, F., Costa, A., Lo Schiavo, F., Pupillo, P., and Trost, P. (2006). Redox regulation of a novel plastid-targeted β-amylase of Arabidopsis. Plant Physiol. **141:** 840–850.

Stitt, M., and Zeeman, S.C. (2012). Starch turnover: pathways, regulation and role in growth. Curr. Opin. Plant Biol. **15:** 282–292.

Streb, S., and Zeeman, S.C. (2012). Starch metabolism in Arabidopsis. Arabidopsis Book **10:** e0160.

Sulpice, R., Flis, A., Ivakov, A.A., Apelt, F., Krohn, N., Encke, B., Abel, C., Feil, R., Lunn, J.E., and Stitt, M. (2014). Arabidopsis coordinates the diurnal regulation of carbon allocation and growth across a wide range of photoperiods. Mol. Plant **7:** 137–155.

Toroser, D., and Huber, S.C. (1997). Protein phosphorylation as a mechanism for osmotic-stress activation of sucrose-phosphate synthase in spinach leaves. Plant Physiol. **114:** 947–955.

Umezawa, T., Sugiyama, N., Mizoguchi, M., Hayashi, S., Myouga, F., Yamaguchi-Shinozaki, K., Ishihama, Y., Hirayama, T., and Shinozaki, K. (2009). Type 2C protein phosphatases directly regulate abscisic acid-activated protein kinases in Arabidopsis. Proc. Natl. Acad. Sci. USA **106:** 17588–17593.

Urano, K., Maruyama, K., Ogata, Y., Morishita, Y., Takeda, M., Sakurai, N., Suzuki, H., Saito, K., Shibata, D., Kobayashi, M., Yamaguchi-Shinozaki, K., and Shinozaki, K. (2009). Characterization of the ABA-regulated global responses to dehydration in Arabidopsis by metabolomics. Plant J. **57:** 1065–1078.

Usadel, B., Bläsing, O.E., Gibon, Y., Poree, F., Höhne, M., Günter, M., Trethewey, R., Kamlage, B., Poorter, H., and Stitt, M. (2008a). Multilevel genomic analysis of the response of transcripts, enzyme activities and metabolites in Arabidopsis rosettes to a progressive decrease of temperature in the non-freezing range. Plant Cell Environ. **31:** 518–547.

Usadel, B., Bläsing, O.E., Gibon, Y., Retzlaff, K., Höhne, M., Günther, M., and Stitt, M. (2008b). Global transcript levels respond to small changes of the carbon status during progressive exhaustion of carbohydrates in Arabidopsis rosettes. Plant Physiol. **146:** 1834–1861.

Valerio, C., Costa, A., Marri, L., Issakidis-Bourguet, E., Pupillo, P., Trost, P., and Sparla, F. (2011). Thioredoxin-regulated beta-amylase (BAM1) triggers diurnal starch degradation in guard cells, and in mesophyll cells under osmotic stress. J. Exp. Bot. **62:** 545–555.

Verslues, P.E., and Sharma S. (2011). Proline metabolism and its implications for plant-environment interaction. The Arabidopsis Book **8:** e0140, doi/10.1199/tab.0140.

Viola, R., and Davies, H.V. (1992). A microplate reader assay for rapid enzymatic quantification of sugars in potato tubers. Potato Res. **35:** 55–58.

Wan, X.-R., and Li, L. (2006). Regulation of ABA level and water-stress tolerance of Arabidopsis by ectopic expression of a peanut 9-cis-epoxycarotenoid dioxygenase gene. Biochem. Biophys. Res. Commun. **347:** 1030–1038.

Wu, Y., and Cosgrove, D.J. (2000). Adaptation of roots to low water potentials by changes in cell wall extensibility and cell wall proteins. J. Exp. Bot. **51:** 1543–1553.

Xue, L., Wang, P., Wang, L., Renzi, E., Radivojac, P., Tang, H., Arnold, R., Zhu, J.-K., and Tao, W.A. (2013). Quantitative measurement of phosphoproteome response to osmotic stress in arabidopsis based on Library-Assisted eXtracted Ion Chromatogram (LAXIC). Mol. Cell. Proteomics **12:** 2354–2369.

Yamaguchi-Shinozaki, K., and Shinozaki, K. (1994). A novel cis-acting element in an Arabidopsis gene is involved in responsiveness to drought, low-temperature, or high-salt stress. Plant Cell **6:** 251–264.

Yamaguchi-Shinozaki, K., and Shinozaki, K. (2006). Transcriptional regulatory networks in cellular responses and tolerance to dehydration and cold stresses. Annu. Rev. Plant Biol. **57:** 781–803.

Yano, R., Nakamura, M., Yoneyama, T., and Nishida, I. (2005). Starch-related α-Glucan/Water Dikinase is involved in the cold-induced development of freezing tolerance in Arabidopsis. Plant Physiol. **138:** 837–846.

Yazdanbakhsh, N., and Fisahn, J. (2011). Mutations in leaf starch metabolism modulate the diurnal root growth profiles of *Arabidopsis thaliana.* Plant Signal. Behav. **6:** 995–998.

Yoshida, T., Fujita, Y., Maruyama, K., Mogami, J., Todaka, D., Shinozaki, K., and Yamaguchi-Shinozaki, K. (2015). Four Arabidopsis AREB/ABF transcription factors function predominantly in gene expression downstream of SnRK2 kinases in abscisic acid signalling in response to osmotic stress. Plant Cell Environ. **38:** 35–49.

Yoshida, T., Fujita, Y., Sayama, H., Kidokoro, S., Maruyama, K., Mizoi, J., Shinozaki, K., and Yamaguchi-Shinozaki, K. (2010). AREB1, AREB2, and ABF3 are master transcription factors that cooperatively regulate ABRE-dependent ABA signaling involved in drought stress tolerance and require ABA for full activation. Plant J. **61:** 672–685.

Yoshida, T., Mogami, J., and Yamaguchi-Shinozaki, K. (2014). ABA-dependent and ABA-independent signaling in response to osmotic stress in plants. Curr. Opin. Plant Biol. **21:** 133–139.

Yu, T.-S., et al. (2005). α-Amylase is not required for breakdown of transitory starch in Arabidopsis leaves. J. Biol. Chem. **280:** 9773–9779.

Zanella, M., Borghi, G.L., Pirone, C., Thalmann, M., Pazmino, D., Costa, A., Santelia, D., Trost, P., and Sparla, F. (2016). β-Amylase 1 (BAM1) degrades transitory starch to sustain proline biosynthesis during drought stress. J. Exp. Bot. **67:** 1819–1826.

Zeller, G., Henz, S.R., Widmer, C.K., Sachsenberg, T., Rätsch, G., Weigel, D., and Laubinger, S. (2009). Stress-induced changes in the *Arabidopsis thaliana* transcriptome analyzed using whole-genome tiling arrays. Plant J. **58:** 1068–1082.

Zhang, W., Ruan, J., Ho, T.H.D., You, Y., Yu, T., and Quatrano, R.S. (2005). Cis-regulatory element based targeted gene finding: genome-wide identification of abscisic acid- and abiotic stress-responsive genes in *Arabidopsis thaliana.* Bioinformatics **21:** 3074–3081.